Journal of Hazardous Materials 501 (2026) 140686

Contents lists available at ScienceDirect

Journal of Hazardous Materials

journal homepage: www.elsevier.com/locate/jhazmat

PFOA and PFOS accumulation induces genotoxic damage and proteomic alterations in *Cannabis sativa* shoots

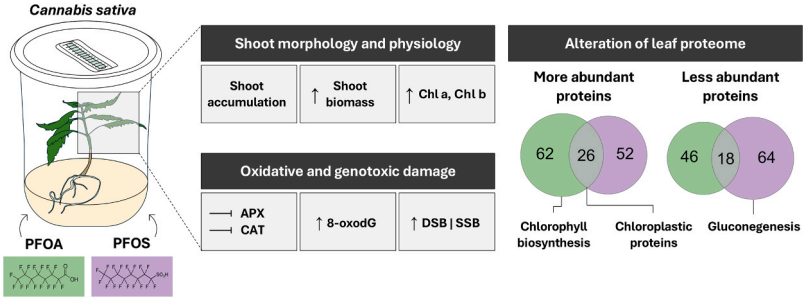
Sophia Luche [a], Alessandra Fanelli [a], Annamaria Buschini [a], Ada Ricci [a], Chiara Maccari [b], Roberta Andreoli [c], Teofilo Vamerali [d], Patrizia Brunetti [e], Giuseppe Capobianco [f], Giovanna Visioli [a,*]

[a] Department of Chemistry, Life Sciences and Environmental Sustainability, University of Parma, Parma 43100, Italy
[b] Centre for Research in Toxicology (CERT), University of Parma, Parma 43126, Italy
[c] Department of Medicine and Surgery, University of Parma, Parma 43126, Italy
[d] Department of Agronomy, Food, Natural Resources, Animals and the Environment (DAFNAE), University of Padua, Legnaro, Padua 35020, Italy
[e] Research Institute on Terrestrial Ecosystems - National Research Council (IRET-CNR), Monterotondo Scalo, Rome 00015, Italy
[f] Department of Chemical Engineering, Materials & Environment, Sapienza University of Rome, Rome 00184, Italy

HIGHLIGHTS

- Exposure to PFOA increased above-ground biomass and chlorophyll content in hemp.
- Exposure to PFOA and PFOS inhibited the activity of antioxidant enzymes.
- PFAS Accumulation induced oxidative damage and compromised DNA integrity.
- PFOA and PFOS alter leaf proteome, affecting specific biological processes.

GRAPHICAL ABSTRACT



ARTICLE INFO

Keywords:
Persistent organic pollutants
PFAS
Plant
Genotoxicity
Comparative proteomics

ABSTRACT

Due to their environmental persistence, widespread application, and toxicity to living organisms, contamination by PFAS has become a significant global concern. The ability of industrial hemp (*Cannabis sativa L.*) to accumulate PFAS in its aerial tissues makes it a candidate for PFAS phytoremediation, as well as a suitable biological model for assessing the toxicological effects of PFAS in higher eukaryotes. After *in vitro* culturing of industrial hemp for 14 days in the presence of 1 mg L^{-1} PFOA or 1 mg L^{-1} PFOS, no visible damage or macroscopic morphological alterations were evident, and a significant increase in shoot biomass and chlorophyll content following PFOA exposure was observed. Despite the higher accumulation of PFOS compared to PFOA both inhibited antioxidant enzymes activity, specifically catalase and ascorbate peroxidase, respectively. Alkaline Comet Assay showed nuclear damage in hemp leaves following both PFOA and PFOS accumulation, with the former significantly increasing 8-oxo-deoxyguanosine formation. Comparative proteomics analyses showed that PFOA and PFOS disrupt specific biological processes, with the former promoting the synthesis of proteins involved in the chlorophyll biosynthetic pathway. Both PFOA and PFOS altered the abundance of chloroplastic

* Corresponding author.
E-mail address: giovanna.visioli@unipr.it (G. Visioli).

https://doi.org/10.1016/j.jhazmat.2025.140686
Received 16 September 2025; Received in revised form 28 November 2025; Accepted 1 December 2025
Available online 1 December 2025
0304-3894/© 2025 The Author(s). Published by Elsevier B.V. This is an open access article under the CC BY license (http://creativecommons.org/licenses/by/4.0/).

proteins, suggesting that this cellular compartment could be involved in the phytotoxicity mechanisms triggered by PFAAs.

1. Introduction

Per- and polyfluoroalkyl substances (PFAS) are synthetic organic compounds containing at least one perfluorinated methyl (-CF_3) or methylene (-CF_2-) group, including more than 7 million different structures [1,2]. These comprise perfluoroalkyl acids (PFAAs), characterized by the presence of a terminal functional group on the perfluorinated alkyl chain, such as a carboxylate in perfluorocarboxylic acids (PFCAs) or a sulfonate in perfluorosulfonic acids (PFSAs). Perfluorooctanoic acid (PFOA), perfluorooctanesulfonic acid (PFOS), and their related compounds have been listed under the Stockholm Convention on Persistent Organic Pollutants (POPs) [1,3]. Indeed, the strength of the C-F bond confers PFAS high thermal and chemical stability; this property, together with their high environmental persistence, has earned them the name "forever chemicals" [4]. PFAS are ubiquitous in the environment due to their widespread use in a wide range of industrial applications, and because of their mobility and tendency to interact with different environmental matrices [5]. A large body of research has highlighted the toxicity of PFAS, with much of this research based on evidence relating to "legacy" PFAS, such as PFOA and PFOS [6]. While the ecotoxicological profiles of PFAS and their detrimental effects on humans, wildlife, and various environmental organisms have been extensively characterized, data regarding their phytotoxic potential remain comparatively scarce [7–9].

Plants, as eukaryotes sharing many cellular and molecular features with animals, represent ideal models for environmental biomonitoring of emerging contaminants, given their direct interaction with all environmental matrices and the ability to detect toxic and genotoxic alterations with high sensitivity and without ethical concerns [10,11]. Toxicological assessments using model plant species have demonstrated the genotoxic capabilities of PFAS, including disruptions of mitotic activity and compromised DNA integrity [12,13]. Phytotoxic responses are strongly influenced by the specific PFAS compound, the plant species involved, and the duration of exposure [14]. To date, a limited number of studies have explored how different structural features (*e.g.* carbon chain length and functional group) determine molecular interactions at cellular and subcellular levels in plant species. A study in tobacco, which compared the toxicity of two PFSAs with different carbon chain lengths, showed that PFOS induced a greater increase in reactive oxygen species (ROS) and malondialdehyde (MDA) content than perfluorobutane sulfonate (PFBS), probably due to the former's ability to interact more strongly and inhibit the activity of antioxidant enzymes such as superoxide dismutase (SOD) and catalase (CAT) [15]. In a study that utilized *Arabidopsis thaliana* mutants to compare the phytotoxicity of PFCAs and PFSAs with the same carbon chain length, it was found that although both PFOA and PFOS modulate the auxin signaling pathway, the disruption of the abscisic acid signaling pathway was PFOS-specific [16]. Metabolomic analyses in hydroponically grown lettuce revealed different targets of PFOA and PFOS phytotoxicity: while exposure to PFOA affects amino acid metabolism, PFOS perturbs linoleic acid metabolism [17].

Several agriculturally relevant species—such as cereals, fruit-bearing plants, and vegetables—have been shown to bioaccumulate PFAAs in their edible tissues. This raises significant public health concerns and underscores the imperative for regulatory oversight by governmental agencies, as well as the urgent development of sustainable strategies to mitigate PFAS environmental dissemination [18–20]. As a Nature-Based Solution that exploits the ability of plants to uptake and accumulate contaminants from the environment, phytoremediation is being studied as a potential strategy for the remediation of PFAS contaminated soils [21]. Industrial hemp has been proven to be a hyperaccumulator of PFAAs [22], and it has been the subject of a pilot-scale PFAS phytoremediation trial [23]. Hemp is a plant species characterized by rapid growth rates, which generally tend to exhibit enhanced PFAS bioaccumulation efficiency, a phenomenon likely attributable to elevated transpiration rates that facilitate the passive upward translocation of these contaminants through the xylem [22–26]. These traits enable hemp to accumulate PFAAs in aerial tissues, primarily in leaves and pollen [23,27], thereby making it also a suitable species for investigating the physiological and molecular responses elicited by PFAS.

This study aimed to employ industrial hemp (*Cannabis sativa* L.) as a model species to investigate potential differential phytotoxicity of PFOA or PFOS exposure, as representatives of PFCAs and PFSAs. At this purpose, *in-vitro* cultured hemp was exposed to a sub-inhibitory concentration of PFOA or PFOS, and their accumulation in aerial parts, variation in biomass production, and content of photosynthetic pigments were evaluated. To assess whether PFAS exposure could perturb oxidative balance in hemp aerial tissues, the activity of two antioxidant enzymes, ascorbate peroxidase (APX) and CAT were also measured. Furthermore, potential genotoxicity of PFOA and PFOS exposure were evaluated in terms of DNA fragmentation and production of oxidative adducts. Finally, we conducted a comparative proteomic profiling to identify common and specific cellular pathways deregulated following PFOA or PFOS exposure. The integration of physiological, ecotoxicological and proteomic data suggests that PFOA, despite accumulating in hemp tissues at significantly lower concentrations than PFOS, induces comparable levels of DNA damage and activates distinct metabolic pathways, highlighting the importance of comparative studies in assessing PFAS genotoxicity.

2. Material and methods

2.1. Chemicals

Two perfluoroalkyl acids were selected as representative of perfluoroalkyl carboxylic acids and perfluoroalkyl sulfonic acids and were used for plant treatment: perfluorooctanoic acid (PFOA) (Sigma Aldrich, St. Louis, MS, USA) and perfluorooctanesulfonic acid (PFOS) (abcr GmbH, Karlsruhe, Germany). Isotopically labelled PFAS standards $^{13}C_4$-PFOA and $^{13}C_4$-PFOS (Wellington laboratories, Guelph, ON, Canada) were added at a fixed concentration as external standards (ES) in mass spectrometry (MS) analysis to perform PFAS identification and quantification. Before use, PFAS stock solutions were vortexed and sonicated for 15 min at room temperature in an Elma Transsonic T460/H (Elma Electronic GmbH, Pforzheim, Germany).

2.2. Allium cepa cytogenotoxicity test

A preliminary cytogenotoxicity test was conducted on onions (*Allium cepa*) grown in deionized water in the dark (25 °C) until a root development of 2–3 cm was observed. Onion roots were then exposed for 48 h to 1, 10, or 25 mg L^{-1} of PFOA or PFOS, or deionized water in the untreated negative control. Following the exposure period, roots were immediately fixed at 4 °C for 24 h with a solution of absolute ethanol: acetic acid (3:1 v/v), and hydrolyzed in 1 M HCl 10 min at 60 °C. The hydrolyzed roots were stained with Schiff's reagent (Sigma Aldrich, St. Louis, MS, USA) for 2 h. Meristematic root tips were then observed and analyzed using a Nikon Eclipse Ci-L Plus Microscope (Nikon Europe BV, The Netherlands) at x40 magnification. Five roots per condition were analyzed, and a minimum of 500 cells were counted for each root. The mitotic index was calculated as the number of mitotic cells divided by the total number of counted cells, multiplied by 100, according to

Sivaram et al. [13].

2.3. Plant growth and treatment

The plant species selected for the study was industrial hemp (*Cannabis sativa* L., monoecious seed variety "Earlina"; SOC, France). Hemp seeds were surface sterilized in 40 % (v/v) commercial bleach. The seeds were plated in ¼ strength Murashige and Skoog nutrient solution (MS, Duchefa Biochimie, Haarlem, The Netherlands), vernalized in the dark at 4 °C for 3 days, and transferred to a controlled growth chamber (25 °C, 16 hr/8 hr light/dark; 120 μmol m^{-2} s^{-1} photosynthetic photon flux, 75 % HR) for germination. Seedlings were then transferred to polypropylene pots (dimensions: 140 mm depth, 120 mm top diameter, 90 mm base diameter) containing ½ strength MS, 0.6 % (w/v) plant agar (Duchefa Biochimie, Haarlem, The Netherlands), 2 % (w/v) sucrose (VWR, Darmstadt, Germany), 1x vitamin mixture (Duchefa Biochimie, Haarlem, The Netherlands), spiked with 1 mg L^{-1} PFOA or 1 mg L^{-1} PFOS. Pots without PFAS supplementation served as control conditions. Three seedlings per pot and four pots per condition were prepared. After 14 days in a controlled growth chamber, plants were sampled for subsequent analyses.

2.4. PFAS extraction and quantification

PFOA and PFOS extraction were performed on dry samples obtained from shoots oven-dried and ground with a mortar and pestle. 0.1 g of dry samples were suspended in 1 mL 50 % MeOH, sonicated for 20 min, and centrifuged 10 min at 14000 rpm. The same procedure was repeated twice, to ensure maximal recovery of PFAS. Both supernatants were combined, filtered through a 0.22 μm CA membrane filter, transferred to Falcon tubes and stored at 4 °C. Before injection samples were diluted in ratio 1:5 and spiked with a ^{13}C-labeled PFOA and PFOS external standard mixture (Wellington Laboratories) to a final concentration of 2 μg L^{-1} for quantification purposes. Concentration levels ranging from 0.01 to 150 ppb of PFOA and PFOS standards were used to determine the linearity of the standard calibration curves. Both PFAAs showed good linearity, with correlation coefficients (R^2) > 0.990. Quantification of molecules was carried out using the corresponding calibration curve. The limit of detection (LoD) and the limit of quantification (LoQ) were defined at a S/N ratio ≥ 3 and S/N ratio ≥ 10, respectively. LoD and LoQ values of PFOA and PFOS were 0.1 ng g^{-1} and 0.2 ng g^{-1}. The accuracy and recovery of PFAS extraction were calculated by using a ^{13}C-labeled internal standard (Wellington Laboratories). PFOA recovery was 87 % meanwhile PFOS resulted 82 %. Liquid chromatography coupled to tandem mass spectrometry (LC- LC-MS/MS) analysis using a triple quadrupole mass spectrometer (TSQ Quantiva, Thermo Fisher Scientific, USA) coupled with ultra-high performance liquid chromatography (Ultimate 3000 UHPLC, Dionex, Thermo Fisher Scientific, USA) was employed to quantify PFOA and PFOS, in accordance with the methodology described by Sharma et al. [28]. Data acquisition was performed in single-reaction monitoring (SRM) mode, and raw data were processed using Skyline MS v. 21.2.0.425.

2.5. Morphological, physiological and biochemical parameters

For shoot biomass quantification, plants were collected from pots and shoot fresh weight was registered and reported as mean weight. Leaf area was measured by analyzing second leaves (n = 6) pictures using ImageJ (version 1.54d). Quantification of chlorophyll a, chlorophyll *b* and carotenoids were performed as reported by Kotecha and Ram [29] with some modifications: 100 mg of frozen leaf tissue was homogenized in 80 % acetone (v/v), centrifuged 5 min at 5000 rpm, and analyzed for pigments content in a Cary 60 Spectrophotometer (Agilent Technologies, Santa Clara, USA). Catalase (CAT) and ascorbate peroxidase (APX) activities were determined according to Potestio et al. [30], with some minor modification. Briefly, 100 mg of frozen leaves were ground in liquid nitrogen, suspended in 500 μL of 50 mM potassium phosphate buffer (pH 7 with 0.1 mM EDTA) and 1 mM phenyl-methane-sulfonyl-fluoride (PMSF). After centrifugation at 14000 rpm at 4 °C for 20 min, supernatant was used to quantify CAT and APX enzyme activity.

2.6. Quantification of 8-oxo-deoxyguanosine

7,8-dihydro-8-oxo-2′-deoxyguanosine (8-oxodG) was quantified on genomic DNA extracted from 100 mg of frozen leaf tissues. DNA was isolated by grinding the tissue in liquid nitrogen to fine powder. Upon liquid nitrogen evaporation, isolation buffer was added (0.3 M NaCl, 50 mM Tris–Cl pH7.5, 20 mM EDTA, 0.5 % SDS). After 5-min incubation at RT, solution was centrifuged at 12000 rpm for 5 min. An equal volume of PCI (Phenol:Chloroform:Isoamyl Alcohol, 25:24:1) was added to supernatant. After centrifugation 12'000 rpm for 10 min at 4 °C, DNA was precipitated adding 0.8 V isopropanol to the upper phase and recovered by centrifugation at 12000 *g* for 10 min at 4 °C. The DNA pellet was washed in 75 % cold ethanol and after brief air-drying, resuspended in water. A nuclease mix that degrades DNA to its individual nucleoside components (DNA Degradase Plus, Zymo Research, CA, USA) was used to digest 4 μg of DNA. Base quantification was performed with UHPLC-MS/MS (ExionLC-API 6500 +, Sciex). Chromatographic separation was done in elution gradient (Phase A 10 mM HCOOH pH 3.75, Phase B MeOH) with column (ATLANTIS C18, Waters). The detection was performed in MRM mode and positive ionization.

2.7. Alkaline comet assay

Alkaline comet assay (or single cell gel electrophoresis) was performed according to Gullì et al. [31] with some modifications. Briefly, plant cell nuclei were obtained from *C. sativa* second leaves directly taken from *in vitro* plants and placed in a 60 mm Petri dish. Using a razor blade, the leaves were sliced perpendicular to the main rid to form a fringe. The cut surface was sprinkled with 200 μL of 0.7 % Low Melting point Agarose (LMA) in Phospate-bufferd saline (PBS) to collect nuclei. Afterwards a 100 μL aliquot of nuclei/agarose mixture was transferred to a glass slide previously coated with 1 % Normal Melting point Agarose (NMA) in PBS, covered with a cover slip and cooled at 4 °C for minimum 15 min. A final layer was obtained using 90 μL of 0.7 % LMA in PBS and cooling again at 4 °C for least 15 min. After gel formation, the cover slip was removed, and the slides were moved to an electrophoresis apparatus. A cold electrophoresis buffer (1 mM Na_2EDTA, 300 mM NaOH, pH ≥ 13) was added and electrophoresis was performed (0.66 V cm^{-1}, 300 mA, 10 min, 4 °C). After electrophoresis, the slide was washed in neutralization buffer (0.4 M Tris-HCl, pH 7.5), fixed 5 min in cold 96 % ethanol and dried at room temperature. Nuclei, stained with 100 μL ethidium bromide (10 μg mL^{-1}), were observed through a fluorescence microscope (Leica DMLS, Leica Microsystem, Wetzlar, Germany) equipped with an excitation filter (BP 515–560 nm) and a barrier filter (LP 580 nm) and linked to a monochromatic camera (Pulnix PE-2020P, Pulnix; Alzenau, Germany). An automatic image analysis system (Comet assay IV; Perceptive Instrument Ltd., Bury St. Edmunds, UK) was used to analyze fifty random selected nuclei per slide. Two slides were analyzed for every tested condition. The tail intensity parameter (median % tail intensity) was selected to estimate DNA damage.

2.8. Sample preparation, LC-MS/MS analysis and data analysis

Protein extraction from fresh leaves was performed as reported by Carpentier et al. [32] with some minor modifications. Powdered tissue was initially homogenized in a buffer containing 0.5 M Tris pH 8.0, 0.7 M sucrose, 0.1 M KCl, 1 % dithiothreitol (w/v), 1 mM phenylmethylsulfonyl fluoride, 1x protease inhibitor cocktail (Roche, Basel, Switzerland) in a 1:4 ratio, before phenol-based extraction and back-extraction. Protein precipitation in ammonium acetate/methanol

was carried out overnight. Protein pellets were washed once with the precipitating solution and three times with cold acetone and resuspended in a buffer made of 7.2 M urea, 90 mM Tris, 2 % SDS (w/v), pH 8.5. Proteins were quantified by BCA assay before tryptic digestion via Filter-Aided Sample Preparation (FASP) method, as described in detail by Battisti et al. [33]. Finally, dried peptide samples were resuspended in 3 % acetonitrile (ACN)/0.1 % formic acid (FA) for LC-MS/MS analysis.

Mass spectrometry analysis was carried out using an Orbitrap Exploris 480 (Thermo Fisher Scientific, Waltham, USA) interfaced with a Vanquish Neo UPLC System (Thermo Fisher Scientific, Waltham, USA). For each sample, 200 ng of peptide mixture were loaded into a trap column (PepMap™ Neo Trap Cartridge, C18, 5 µm, 300 µm x 5 mm, Thermo Fisher Scientific, Waltham, USA) and separated using an Aurora Elite XT UHPLC analytical column (C18, 1.7 µm, 75 µm x 150 mm, IonOpticks) with a linear gradient of ACN/0.1 % FA from 3 % to 25 % in 60 min using a flow rate of 250 nl/min. Column temperature was fixed at 50 °C, ion transfer tube temperature was set at 280 °C, spray voltage was fixed at 1.8 kV, and AGC target and RF lens values were set to 300 % and 50 %, respectively. The instrument operated in a data-dependent mode, with a full scan at 60000 resolution in the 300–1200 *m/z* range, followed by MS/MS scans of the 20 most intense ions at 15000 resolution. Three biological and three technical replicates were acquired for each sample.

Protein search was performed with MaxQuant [34] software v.2.5.2.0. against the *C. sativa* database (UniProt UP000583929, version 2025–04–14, 30192 sequences). Trypsin was set as enzyme with up to 2 missed cleavages allowed, while cysteine carbamidomethylation and methionine oxidation were set as fixed and variable modifications, respectively. A minimum of two peptides was required for protein identification, and results were filtered considering a false-discovery rate (FDR) of 0.01, both at the peptide and protein levels. Data normalization (Cyc-Loess) and statistics (Limma moderated *t*-test) were carried out using NormalyzerDE v.1.14 [35]. Differences in the protein abundance were considered significant at AdjP $\leq$ 0.05 using a fold change (FC) threshold of ±1.2. A classification based on clusters of orthologous groups (COGs) was performed on differentially abundant proteins (DAPs) identified following exposure to PFOA or PFOS (*vs* untreated control), using eggNOG-mapper [36]. Enrichment analysis ($p < 0.05$; Benjamini<0.05) was performed using the DAVID Bioinformatics Database (https://david.ncifcrf.gov/). DAVID default annotation categories were condensed in 3 groups: Biological Process (UP_KW_BIOLOGICAL_PROCESS, GOTERM_BP_DIRECT), Cellular Component (UP_KW_CELLULAR_COMPONENT, GOTERM_CC_DIRECT), and Pathway (KEGG_PATHWAY). Bidirectional bar chart, Venn diagrams, chord diagram, and functional annotation chart bubble plots were generated with R Studio (version 2025.05.0, build 496; https://www.R-project.org/) *eulerr*, *ggplot2*, and *circlize* packages [37–39].

3. Results

3.1. Determination of sub-toxic PFOA and PFOS concentrations

To identify the concentration of PFAS suitable for evaluating possible effects on DNA without affecting the growth capacity of plants, preliminary tests were carried out on *Allium cepa*, commonly used as a model species for environmental monitoring. *A. cepa* roots were exposed to increasing concentrations of PFOA and PFOS (1–25 mg L^{-1}) and the mitotic index in root meristematic cells was evaluated, which is generally considered to be a genotoxic endpoint [13]. The analysis showed that a concentration of 1 mg L^{-1} of either PFOA or PFOS in the growth medium did not result in significant changes to the mitotic index while exposure to concentrations equal to or greater than 10 mg L^{-1} of either PFOA or PFOS led to a drastic reduction in root mitotic index. For this reason, we decided to expose *C. sativa to* 1 mg L^{-1} PFOA or PFOS concentrations in our growth medium (Fig. 1).

3.2. Morphological and physiological parameters of hemp exposed to PFOA and PFOS

After 14 days exposure of hemp plants grown *in vitro* in presence of PFOA or PFOS, concentration of PFAS in aerial tissues and the effect on shoot biomass and pigments contents were assessed as primary end-out of PFAS exposure (Fig. 2). Both PFOA and PFOS were detected in hemp aerial tissues (Fig. 2A). Even though both showed a high accumulation of PFAS in aerial parts of the plants, in terms of micrograms per grams of dry weight (DW), PFOS showed a higher accumulation compared to PFOA in hemp shoots, with a concentration of 43.7 ± 2.5 and 7.8 ± 1.2 µg per grams of DW, respectively. Neither PFOS nor PFOA negatively affected hemp growth, with PFOA exposure significantly increasing shoot biomass, while no differences were observed after PFOS treatment, respect to the control condition (Fig. 2B-2D). Quantification of photosynthetic pigments, including chlorophyll a, chlorophyll *b* and carotenoids, showed that PFOA increased significantly chlorophyll a and b content in hemp leaves while no significant increase was observed after PFOS treatment respect to control condition (Fig. 2F, G). No variation in carotenoids content was observed following both PFOA and PFOS exposure respect to control condition (Fig. 2H).

3.3. Activity of antioxidant enzymes in hemp exposed to PFOA and PFOS

Following 14-day exposure to PFOA or PFOS, activity of two

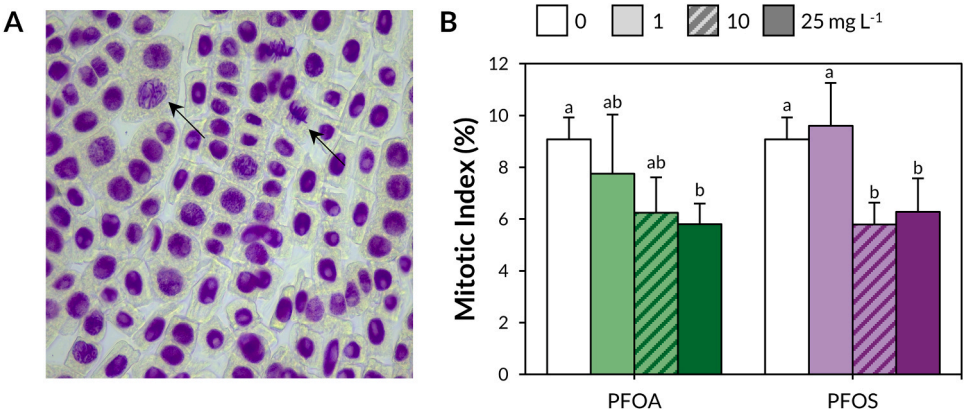


Fig. 1. Analysis of mitotic index in *Allium cepa* meristematic root cells exposed to PFOA or PFOS. (A) Examples of mitotic phases (*black arrows*) identified in *Allium cepa* meristematic cells. (B) Mitotic index (%) variations following exposure to increasing concentration (1–25 mg L^{-1}) of PFOA or PFOS. Average mean values (±SD). Different letters represent significant differences among treatments. (One-way ANOVA followed by a *post hoc* Tukey's test; $p < 0.05$).

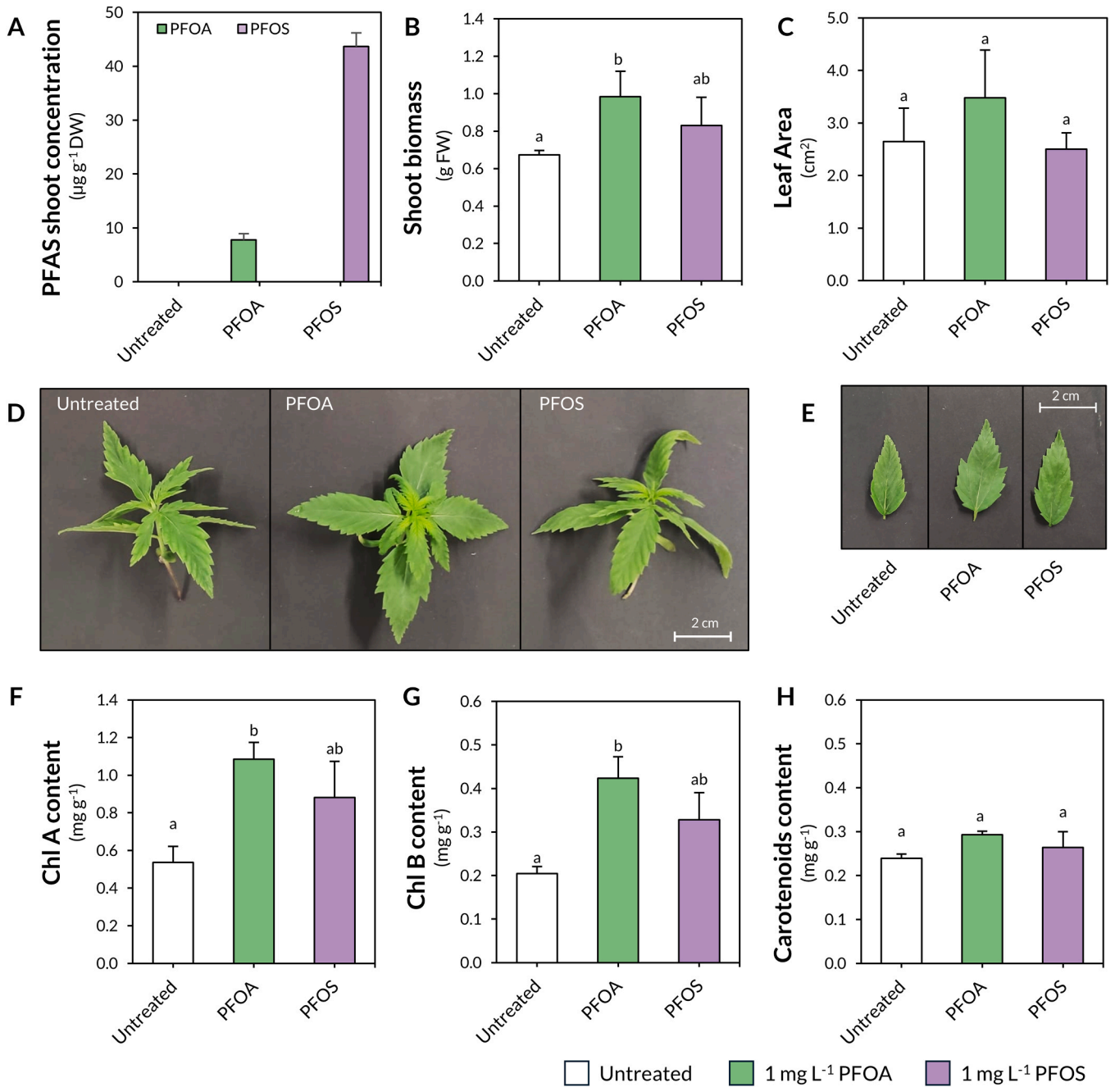


Fig. 2. Shoot quantification of PFAS and their effects on hemp shoot biomass and photosynthetic pigments following 14-days exposure to 1 mg L^{-1} PFOA or PFOS. (A) Concentration of PFOA and PFOS in hemp aerial tissues in terms of µg per grams of dry weight (DW). (B) Quantification of shoot biomass expressed as fresh weight (FW). (C) Hemp leaf area following PFOA or PFOS exposure (n = 6). (D-E) Morphology of *C. sativa* shoots and leaves exposed to PFAS (scale bar, 2 cm). (F-H) Quantification of chlorophyll (Chl) *a*, chlorophyll *b* and carotenoids in hemp leaves. Average mean values (±SD). Different letters represent significant differences among treatments. (One-way ANOVA followed by a *post hoc* Tukey's test; $p < 0.05$).

antioxidants enzymes, APX and CAT were evaluated in hemp leaves (Fig. 3). Results showed that both PFOA and PFOS exposure reduced antioxidant enzymes activity and that the inhibition is PFAS-specific: while a strong decrease in APX activity has been observed after PFOA exposure (Fig. 3A), PFOS induced a decrease in CAT activity (Fig. 3B).

3.4. Oxidative DNA damage in hemp exposed to PFOA and PFOS

Quantification of 8-oxodG and alkaline comet assay were performed to assess whether the exposure to PFOA and PFOS could induce genotoxic alterations in *C. sativa* leaves (Fig. 4). The analysis revealed that after 14 days of exposure, both PFOA and PFOS increased the number of 8-oxodG in genomic DNA respect to the control condition, although for PFOS the effect was not statistically significant (Fig. 4A). In addition, analyses of nuclei extracted from hemp leaves revealed a significant higher degree of DNA migration following exposure to both PFAS, indicating an increase of DNA fragmentation following 14-day exposure to either PFOA or PFOS (Figs. 4B, 4C).

3.5. Comparative proteomic analyses of hemp plants exposed to PFOA and PFOS

A comparative proteomic analysis was conducted to investigate common and specific proteomic pathways deregulated by the

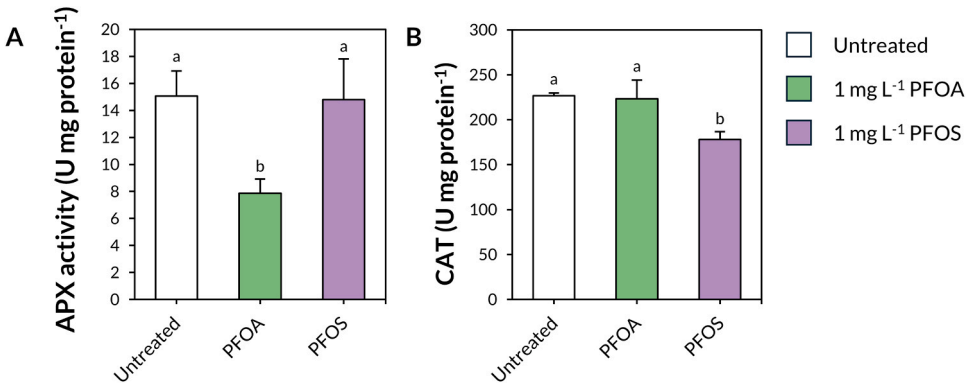


Fig. 3. Evaluation of antioxidant enzymes activity following PFAS exposure. Quantification of ascorbate peroxidase (APX) (A) and catalase (CAT) (B) activity in hemp leaves exposed to 1 mg L^{-1} PFOA or 1 mg L^{-1} PFOS for 14 days. Average mean values (±SD). Different letters represent significant differences among treatments. (One-way ANOVA followed by a *post hoc* Tukey's test; $p < 0.05$).

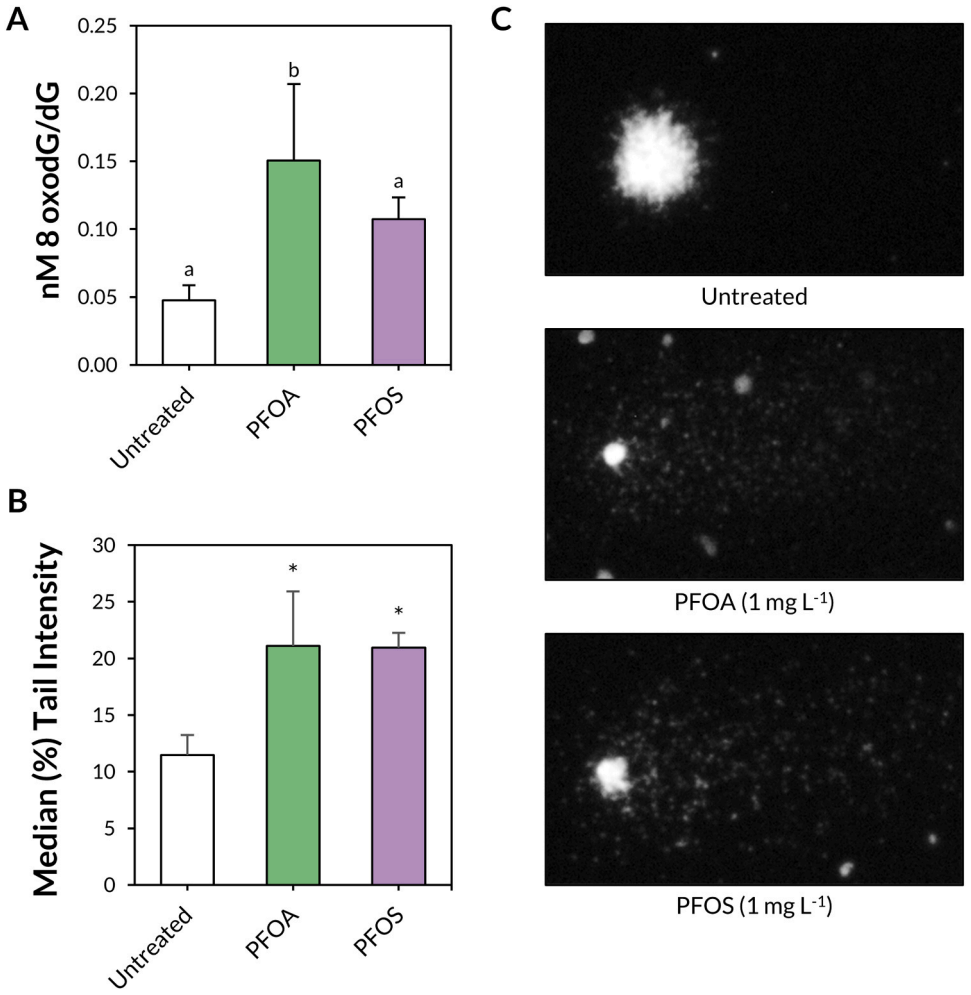


Fig. 4. DNA damage induced by PFOA and PFOS exposure. (A) Quantification of 7,8-dihydro-8-oxo-2′-deoxyguanosine (8-oxodG) on DNA extracted from hemp leaves digested to its individual nucleotides. (B) Median tail intensity (%) (50 nuclei, duplicate slide) from alkaline comet assay on *C. sativa* leaf nuclei. (Test T; *, $p < 0{,}05$; ***, $p < 0{,}001$). (C) Comet images of nuclei extracted from *C. sativa* leaves untreated and treated with 1 mg L^{-1} PFOA or 1 mg L^{-1} PFOS.

accumulation of PFOA or PFOS in *C. sativa* leaves (Fig. 5, Fig. 6, Table S1). A total of 152 and 160 DAPs were identified for PFOA and PFOS, respectively (Table S1). Of these, 88 proteins for PFOA and 78 for PFOS were found to be more abundant with respect to the untreated control while 64 proteins and 82 proteins were found to be less abundant, respectively (Fig. 5A). The most abundant protein following PFOA exposure was a Jacalin-type lectin domain-containing protein (A0A7J6FJ85, Log_2FoldChange = 4.12), whereas for PFOS was a SCP domain-containing protein (A0A7J6GGJ0, Log_2FoldChange = 2.35) (Table S1). The COGs classification of DAPs (Fig. 5B) revealed that for both PFOA and PFOS "Metabolism" was the most affected COG group, with 62 e 69 DAPs, respectively. However, for PFOA most of them were

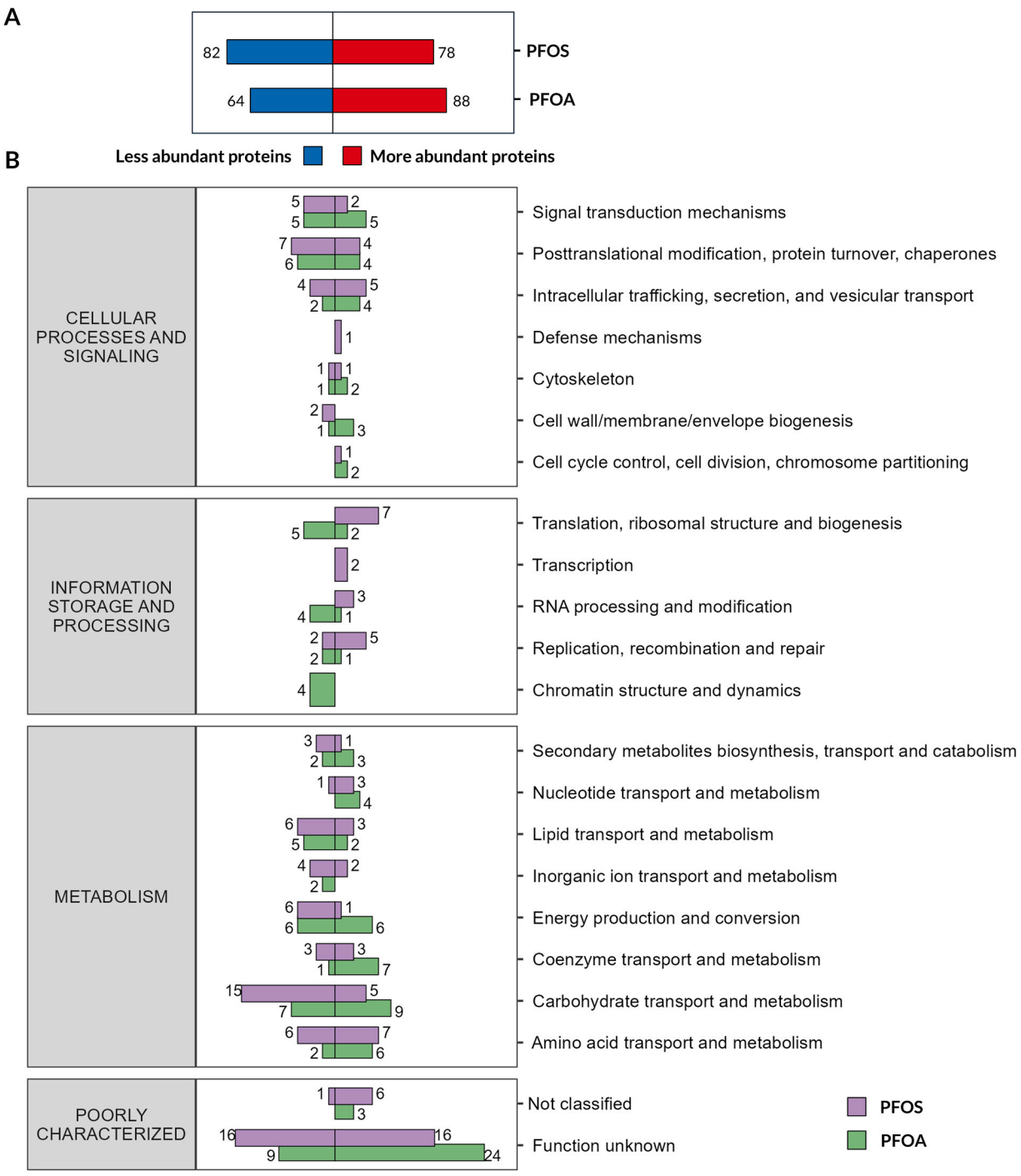


Fig. 5. Overview of differentially abundant proteins identified after exposure to PFOA or PFOS. Bidirectional bar plots showing the number of less abundant proteins (*blue*) and more abundant proteins (*red*) (A) identified after PFOA (*green*) and PFOS (*violet*) treatment, and their clusters of orthologous groups (COGs) - based classification (B).

more abundant proteins (n = 37), while for PFOS were less abundant proteins (n = 44) compared to the untreated control. Categories such as "Carbohydrate transport and metabolism" (n = 16), "Energy production and conversion" (n = 12), and "Amino acid transport and metabolism" (n = 8), were the most represented COGs categories for PFOA, whereas for PFOS were "Carbohydrate transport and metabolism" (n = 20), "Amino acid transport and metabolism" (n = 13), and "Lipid transport and metabolism" (n = 9). Globally, 18 less abundant proteins were common for both PFOA and PFOS exposure, and 26 were common between more abundant proteins (Fig. 6A). Common DAPs belonged to 14 COGs categories (Fig. 6B), and the most represented included "Function unknown" (n = 9), "Amino acid transport and metabolism" (n = 6), and "Carbohydrate transport and metabolism" (n = 5). Functional annotation analysis of DAPs revealed that exposure to both PFAS induced an increase of proteins localized to cellular components such as plastids, specifically chloroplast and chloroplast stroma (Fig. 6C), although most enriched annotation terms were PFAS-specific. PFOA exposure induced a significant increase in proteins involved in crucial step of chlorophyll biosynthetic processes (Figs. 6C, 6D), including a glutamyl-tRNA reductase (A0A7J6H526), two magnesium chelatases (A0A7J6EE54, A0A7J6HU76), a divinyl chlorophyllide a 8-vinyl-reductase (A0A7J6HEK8), and a NADPH-protochlorophyllide oxidoreductase

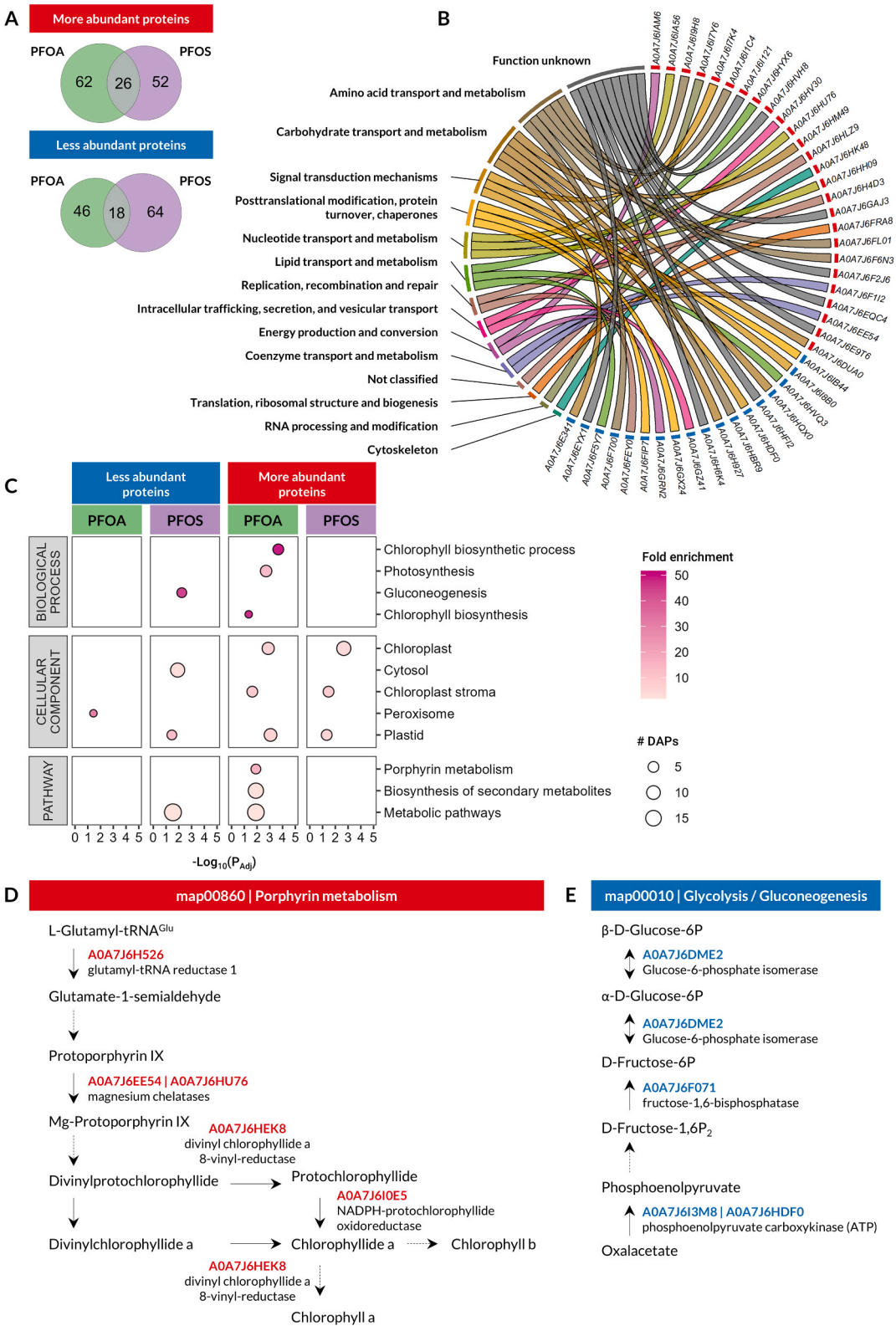


Fig. 6. Comparison of less abundant and more abundant proteins identified following PFOA or PFOS exposure. (A) Venn diagrams showing the overlap of more abundant (*top*) and less abundant proteins (*bottom*) between DAPs identified in PFOA and PFOS treatments. (B) COGs-based classification of less abundant (*blue*) and more abundant proteins (*red*) identified after both PFOA or PFOS exposure. (C) Bubble plot of enriched annotation terms (Benjamini-adjusted $p < 0.05$) of less abundant (*left*) and more abundant proteins (*right*), identified using DAVID Bioinformatics and grouped into Biological Process, Cellular Component, Pathway and Protein features. Fold enrichment and number of DAPs associated with each annotation terms are also reported.
(a) (D) Proteins found to be more abundant after PFOA exposure and involved in chlorophyll biosynthetic processes illustrated within the KEGG Porphyrin metabolism pathway (adapted from map00860). (b) (E) KEGG orthology Glycolysis/Gluconeogenesis pathway illustrating the role of proteins less abundant following PFOS exposure and involved in gluconeogenesis (adapted from map00010).

(A0A7J6I0E5), together with an overabundance of a chloroplastic chlorophyll a-b binding protein (A0A7J6I6H8) (Table S1). Conversely, PFOS exposure determined a decrease in abundance of proteins with roles in gluconeogenesis (Figs. 6C, 6E), such as two phosphoenolpyruvate carboxykinases (A0A7J6I3M8, A0A7J6HDF0), a fructose-1,6-bisphosphatase (A0A7J6F071), and a glucose-6-phosphate isomerase (A0A7J6DME2). Proteins involved in redox processes or in oxidative stress defense were found to be more abundant in the presence of both PFOA and PFOS, and these included a 2Fe-2S ferredoxin-type domain-containing protein (A0A7J6IAM6) and thioredoxin clot (A0A7J6EQC4). Other proteins were PFAS-specific, such as a peroxidase (A0A7J6HPV5) and of a dehydroascorbate reductase (A0A7J6GNZ6), which were more abundant following PFOA exposure; and a Cu-Zn superoxide dismutase (A0A7J6G1D4), the abundance of which increased after PFOS exposure.

4. Discussion

4.1. PFOA and PFOS accumulation promoted hemp growth and chlorophyll content

The ability of industrial hemp to bioaccumulate PFAS in aerial tissues makes it of great interest not only in the context of PFAS phytoremediation [22,23,27] but also as a potential model species for the evaluation of PFAS phytotoxicity and genotoxicity. The aim of this study was to explore the potential effects induced in *in vitro*-grown industrial hemp by the exposure to 1 mg L^{-1} PFOA or PFOS, a concentration that allowed the detection of molecular alterations under short-term exposure without compromising plant growth (Fig. 1, Fig. 2). In addition, this concentration is representative of environmental scenarios characterized by elevated PFAS contamination, such as areas adjacent to fluorochemical industries or sites impacted by the application of aqueous film-forming foams (AFFFs), where PFAS concentrations can reach the ppm range [40,41]. PFAS quantification in hemp shoots showed greater PFOS accumulation compared to PFOA (Fig. 2A). PFAS uptake in plants depends on molecular properties, initial concentrations, species-specific traits, and the physical–chemical characteristics of the root-associated matrix (e.g., liquid vs. solid media) [21,42–44]. Most studies assessing PFAS accumulation in aerial tissues use mixtures, where competitive or interactive effects can alter bioavailability [21,45]. Table S2 summarizes studies measuring PFOA or PFOS in aerial tissues after exposure to individual compounds with all other experimental conditions held constant. Some species, such as cucumber, carrot, lettuce, sea rush, and water hyacinth, accumulate more PFOA, whereas others, including pumpkin and maize, accumulate significantly more PFOS [17,46–51]. No studies on hemp have tested accumulation after exposure to single PFAS. As root PFAS accumulation was not considered in our study, we can only speculate whether differential shoot accumulation among PFOA and PFOS reflects distinct translocation patterns or differences in uptake kinetics influenced by the exposure medium (e.g., plant agar).

Despite their different accumulation profiles, both PFAS induced an increase in above-ground hemp biomass, significantly PFOA, with this latter also promoting an increase in leaf area (Figs. 2B, 2C). It has been proved that low concentrations of PFAS tend to stimulate plant growth, and this phenomenon has been observed in a variety of plant species exposed to different types of PFAAs [20]. Indeed, several studies demonstrate that exposure concentrations of PFOA or PFOS in the growing medium comparable to those utilized in the present study (1 ppm) induce an increase in aboveground tissues in multiple herbaceous species. In hydroponically cultivated maize, an increase in shoot biomass was observed following a 10-day exposure to 1 mg L^{-1} PFOA [50]. In a similar study with *Brassica juncea*, a 7-day exposure resulted in a doubled shoot biomass [52]. Furthermore, an increase in aboveground biomass has been observed in multiple lettuce cultivars following exposure to PFOA or PFOS [53,54]. The phenomenon of plant growth stimulation at low concentrations of chemicals has been observed for pollutants, herbicides, and heavy metals [55–57]. Despite the absence of comprehensive elucidation of the underlying mechanisms of hormesis in plants, emerging evidence suggests a potential involvement of hormonal regulation systems, antioxidant enzymes activity, ROS and stress proteins production in response to exposure to low concentrations of chemicals [58,59]. Furthermore, a meta-analysis by Agathokleous et al. [60] suggested that chlorophylls can be stimulated by abiotic stresses, and can be considered as major components of plant stress biology. Our results showed that both PFOA and PFOS stimulated chlorophyll *a* and chlorophyll *b* content, significantly the former, without affecting carotenoids content (Fig. 2 F-H). An increase in total chlorophyll content was already observed in wheat exposed to increasing concentration (0.1 – 100 μM) of PFOS [61]. Interestingly, bell-shaped responses in chlorophyll content were observed in the aquatic species *Vallisneria natans* and *Cyperus alternifolius* following exposure to increasing concentration of PFOA (0.1–10 μg L^{-1}) or PFOS (0.001–10 mg L^{-1}), respectively [62,63].

4.2. PFOA and PFOS inhibited antioxidants enzymes activity and induced DNA damage

A hallmark of PFAS-induced phytotoxicity is the alteration of cellular antioxidant systems, leading to an increase in ROS and reactive nitrogen species (RNS), often accompanied by damage such as lipid peroxidation, protein oxidation and compromised DNA integrity [64,65]. Consequently, the activity of two antioxidant enzymes, APX and CAT, was evaluated, whose importance in downstream ROS detoxification processes as H_2O_2-metabolising enzymes in plants exposed to abiotic stress is well documented [66]. PFOA and PFOS accumulation in the aerial tissues of hemp resulted in a decrease in the activity of these two antioxidant enzymes (Fig. 3). Specifically, exposure to PFOA was found to reduce APX activity by 50 % (Fig. 3A), and a substantial decrease in CAT activity was observed following exposure to PFOS (Fig. 3B). The inhibition of APX activity following exposure to PFOA (100 μM) has previously been demonstrated in the model plant *A. thaliana*, where, in parallel, a downregulation of gene expression was recorded [67]. Moreover, studies conducted on wheat, soybean, and mung bean revealed a decrease in CAT activity following exposure to PFOS [61,68,69]. It has been hypothesized that PFOA and PFOS may physically interact with antioxidant enzymes, thereby altering the intracellular redox state [70–72]. Specifically, a study that utilized a range of spectroscopic methodologies, molecular docking, and enzymatic activities to assess the binding between PFOA or PFOS and CAT revealed that while the PFOA-CAT interaction is superficial and does not involve alterations in enzyme activity, PFOS binds in proximity to amino acids in the active site, resulting in a 71.81 % decrease in enzyme activity [71]. This evidence suggests that the inhibition of CAT activity observed in hemp leaves following PFOS accumulation may be attributable to PFOS physical interaction and block of enzyme activity. Although the interaction of PFOA with APX has yet to be explored, a similar mechanism could occur. Following exposure to both PFOA and PFOS, the inhibition of antioxidant enzymes could result in ROS accumulation. Indeed, the quantification of 8-oxodG on DNA extracted from hemp leaves following PFAS accumulation, a marker of DNA oxidative damage, showed an increase in oxidative adducts for PFOA and PFOS, with the increase being significant for the former (Fig. 4A). Despite the documented increase in 8-oxodG in plants exposed to heavy metals and salt stress [73,74], a limited number of studies investigated this trait in response to PFAS exposure. In hydroponically cultivated lettuce leaves, an increase in 8-oxodG has been reported through a metabolomic approach following 28-day exposure to 500–5000 ng L^{-1} PFOA or PFOS [75]. Interestingly, a number of cross-sectional studies have correlated human exposure to PFOA and PFOS with an increase in urinary 8-oxodG [76–78]. In order to assess whether the increase in oxidative DNA damage was accompanied by impaired genomic DNA integrity, an alkaline comet assay was performed on nuclei extracted from hemp leaves following 14-day exposure to PFOA or PFOS (Fig. 4B-4C). The

analysis demonstrated a decrease in DNA integrity following exposure to both PFAS, with a significant increase in tail intensity (Fig. 4B) and DNA migration (Fig. 4C) across both treatments. To date, studies employing this technique to detect PFAS genotoxicity in plants are limited to tests conducted in the model species *Allium cepa* [13,79,80]. These studies have demonstrated that exposure to class B firefighting foams, which constitute a primary source of PFAS contamination [81], or to PFOS, results in DNA damage, with a significant increase in tail intensity together with the detection of different chromosomal aberrations, including micronuclei [13,79]. Furthermore, comet assay has been utilized to assess the genotoxicity of PFOA and PFOS in the ecotoxicological model species *Daphnia carinata*, showing significant DNA damage after exposure to 1 mg L^{-1} PFOS or 10 mg L^{-1} PFOA, suggesting a higher genotoxic effect for the former [82]. Furthermore, studies in HepG2 cells exposed to a range of PFAAs have highlighted the genotoxic potential of both PFOA and PFOS, with a significant increase of percentage tail DNA at concentration as low as 1.85 μM and 0.77 μM, respectively [83,84]. In our study, PFOA was detected at lower concentrations than PFOS in hemp aerial tissues (Fig. 2A). Nevertheless, it exerted a stronger intrinsic toxicity, resulting in oxidative and genotoxic damage comparable to those induced by PFOS. This evidence suggests that the observed increase in biomass and chlorophyll content (Figs. 2B, 2F-2G) should not be considered as an adaptive response, but rather as a overcompensatory growth response triggered by a deregulation of cellular homeostasis [85].

4.3. PFOA and PFOS altered hemp leaf proteome

Following PFOA and PFOS accumulation in hemp leaves, a comparative proteomic approach was conducted to assess potential alterations in proteome caused by PFAS exposure (Fig. 5, Fig. 6, Fig. 7, Table S1). Most of the identified DAPs after PFOA or PFOS exposure, a

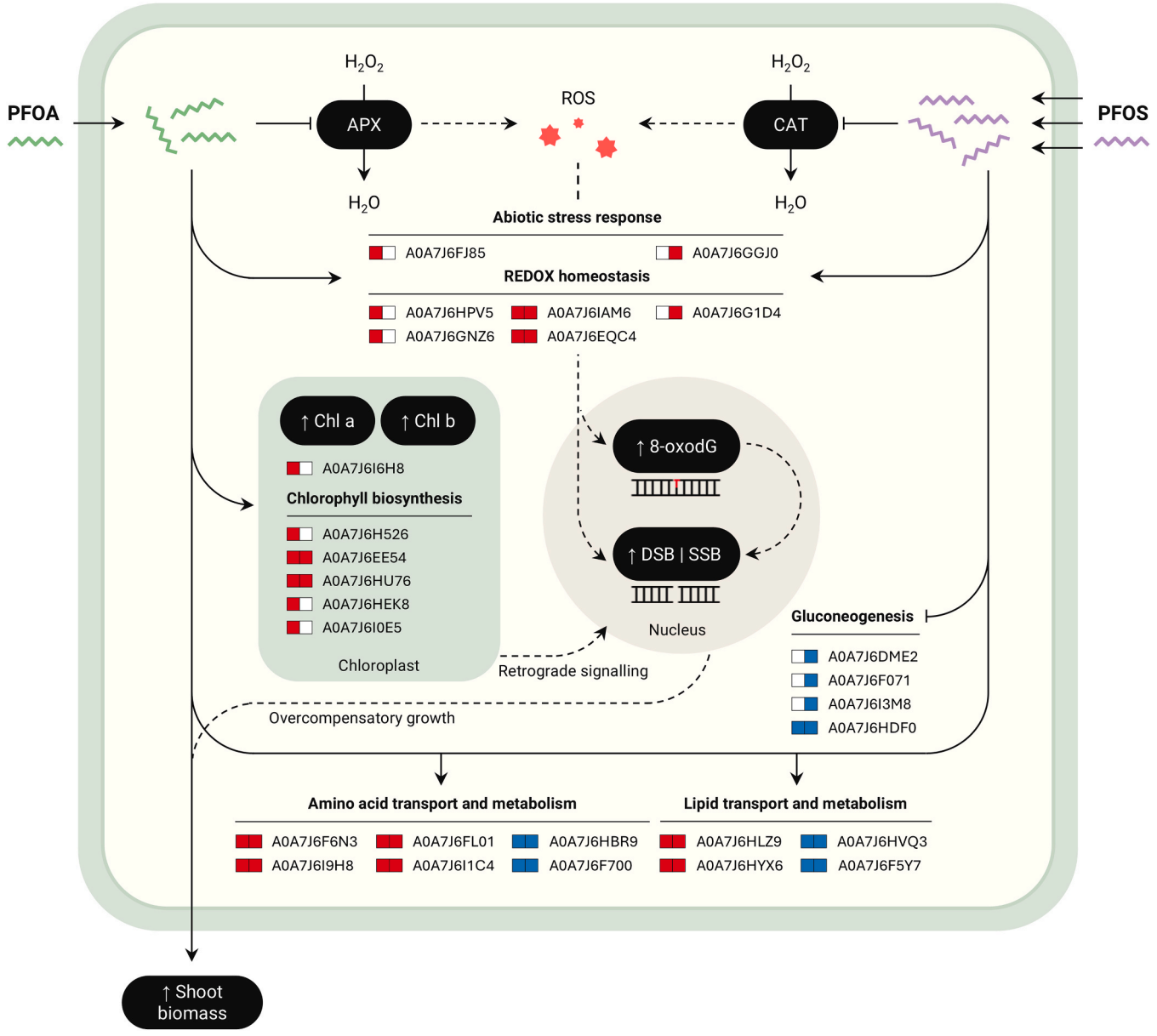


Fig. 7. Schematic overview of the main molecular targets of PFOA- and PFOS-induced phytotoxicity in hemp leaves. Representation of biological processes altered following PFAS exposure, along with the list of specific DAPs involved and their hypothesized interplay (*dotted lines*) with physiological and genotoxic findings, labeled in black square. Lower abundance (*blue*), unaltered (*white*) or higher (*red*) abundance of each DAP following exposure to PFOA (*left*) or PFOS (*right*) is represented by colored squared flanking protein UniProt ID.

significant portion of which being common to both PFAAs (Fig. 6A), belonged to the "Metabolism" COGs category class, mainly related to lipids, amino acids, and carbohydrates transport and metabolism, and in energy production and conversion processes (Fig. 5B).

Given their structural similarity to fatty acids, it is not surprising that the abundance of several proteins involved in lipid metabolism was altered following exposure to PFOA (n = 12) or PFOS (n = 7) (Fig. 5B). Specifically, three of these (A0A7J6HYX6, A0A7J6HVQ3, A0A7J6F5Y7) were found to be commonly altered following exposure to both PFAAs. Moreover, both PFOA and PFOS exposure resulted in an overabundance of a non-specific lipid-transfer protein (A0A7J6HLZ9) (Fig. 6B). In a proteomic analysis of hydroponically grown maize exposed to a mix of PFCAs and PFSAs, the non-specific lipid transfer protein 1 (NSLTP1), involved in fatty acid and lipid metabolism, emerged as one of the most abundant proteins in response to PFAS exposure [86]. Molecular docking analyses further revealed a higher affinity for the tested PFAS compounds compared to the native ligand palmitic acid. The authors also highlight how the high binding affinity of PFOA and PFOS may be due to multiple polar interactions they could form with palmitic acid [86]. Although further analyses would be required to confirm this scenario in hemp, it is possible that, as observed for maize, the binding of PFOA and PFOS to this protein may induce its overproduction in an attempt to restore its ability to perform its physiological functions.

The link between PFAS and altered amino acid metabolism has already been highlighted in several studies that have used metabolomic approaches to analyze the plant response to PFAS exposure. Nevertheless, both increases and decreases in amino acid content were observed, with highly plant-specific and PFAS-specific results [87–91]. The aminoacidic profile of root maize following exposure to a mix of 11 PFAAs was analysed, and the level of 15 amino acids resulted significantly altered. In this study, the abundance of 6 proteins (A0A7J6FL01, A0A7J6I1C4, A0A7J6F6N3, A0A7J6I9H8, A0A7J6HBR9, A0A7J6F700) with roles in amino acids transport and metabolism was found to be altered both in the presence of PFOA or PFOS (Fig. 6B). Interestingly, these include the chorismate synthase (A0A7J6FL01), which was found to be highly over-abundant in response to both PFAAs. This enzyme catalyzes the last step in the shikimate pathway that leads to chorismate production, a precursor molecule for the biosynthesis of aromatic amino acids, such as phenylalanine, tyrosine, and tryptophan, as well as secondary metabolites such as vitamin K, folate and salicylic acid [92]. Co-exposure to PFOA and PFOS in hydroponically grown lettuce resulted in a strong induction of shikimate pathway, and the same trend was observed in PFOS-exposed *A. thaliana* leaves, suggesting this mechanism to be a strategy to cope with PFAS phytotoxicity [88,93].

Several studies have highlighted marked alterations related to carbohydrate metabolism, such as TCA cycle, glycolysis, and gluconeogenesis, following exposure to PFAS in plants [87,89–91]. In this study, hemp exposure to PFOS resulted in a significant reduction in the abundance of proteins involved in gluconeogenesis, compared to the untreated control (Fig. 6C). Covering many steps leading to the synthesis of glucose-6P from oxaloacetate, these proteins included glucose-6-phosphate isomerase (A0A7J6DME2), fructose-1, 6-bisphosphatase (FBP) (A0A7J6F071), and two phosphoenolpyruvate carboxykinases (PEPCK) (A0A7J6I3M8, A0A7J6HDF0) (Fig. 6E). The deleterious effects of PEPCK deficiency have been well documented in several plant species, suggesting a key role in the response to abiotic stresses [94–96]. The downregulation of PEPCK and FBP had previously been associated with the response to light deprivation in grape berries, as key genes controlling gluconeogenesis, thus resulting in lower glucose and fructose levels [96]. A decrease in sugar content has already been observed following exposure to increasing concentrations (0.2–5 mg kg^{-1}) of PFOS in wheat [97]. The inhibition of gluconeogenesis in response to PFOS exposure could therefore represent a metabolic reprogramming towards less energy-consuming processes to cope with the stress generated by its accumulation in tissues, with consequences that could also have an impact on nutritional quality when exposure occurs in edible plants.

The disruption of energy balance processes is another common feature identified in plants exposed to PFOA or PFOS, in which changes in photosynthesis, in terms of fluorescence parameters, gas exchange, and chlorophyll content, are frequently identified [20]. Here, photosynthesis and chlorophyll biosynthetic processes were the most affected biological process following hemp exposure to PFOA (Fig. 6C). Indeed, 5 proteins were found to be significantly more abundant following PFOA accumulation in hemp leaves, which included glutamyl-tRNA reductase 1 (A0A7J6H526), magnesium chelatases (A0A7J6EE54, A0A7J6HU76), divinyl chlorophyllide a 8-vinyl-reductase (A0A7J6HEK8), and NADPH-protochlorophyllide oxidoreductase (A0A7J6I0E5), enzymes that catalyse several step that lead to chlorophyll a and chlorophyll *b* synthesis from L-glutamyl-tRNA. Furthermore, PFOA exposure was found to induce the synthesis of a chloroplastic chlorophyll a-b binding protein (A0A7J6I6H8) (Table S1). This finding aligns with the significant increase in chlorophyll *a* and chlorophyll *b* content observed following PFOA exposure (Fig. 2F-2G). Moreover, tetrapyrroles are known to play a role in oxidative stress-induced cellular response, contributing to ROS-mediated retrograde signalling from plastid affecting nuclear gene expression [98,99]. Here, chloroplasts represented the most affected cellular compartments after both PFOA and PFOS exposure (Fig. 6C), with enzymes such as the magnesium chelatases (A0A7J6HU76, A0A7J6EE54) over-abundant in both treatments. Specifically, these enzymes lead to the formation of Mg-protoporphyrin IX, which is directly involved in retrograde signalling via $^1O_2$ generation following its accumulation [100].

The presence of proteins such as 2Fe-2S ferredoxin-type domain-containing protein (A0A7J6IAM6) and thioredoxin clot (A0A7J6EQC4) (Fig. 6B) among the proteins common to both PFAS supports a scenario of redox imbalance. However, exposure to PFOA or PFOS revealed also specific features. Following exposure to PFOA, the most abundant protein compared to the control was a Jacalin-type lectin domain-containing protein (A0A7J6FJ85) (Table S1). Recently, the role of jacalin-related lectins in abiotic stress response in tomato has been highlighted, along with a chromosomal localization associated with *cis*-regulatory elements involved in environmental stress response [101]. In rice, a salt stress-responsive jacalin-related lectin (*OsJRL45*) was found to improve salt stress tolerance by increasing the activity of antioxidant enzymes and regulating osmotic balance [102]. On the other hand, the most abundant protein compared to untreated control condition following PFOS exposure was a cysteine-rich secretory protein-related protein (A0A7J6GGJ0) (Table S1). It has been proposed that this superfamily domain may participate in abiotic stress tolerance by regulating membrane stability and modulating antioxidant enzyme activity [103]. Interestingly, PFOA and PFOS induced an overabundance of specific antioxidants. Indeed, the former increased the abundance of a peroxidase (A0A7J6HPV5) and of a dehydroascorbate reductase (A0A7J6GNZ6), further supporting the idea of a perturbation of H_2O_2 detoxification systems induced by PFOA exposure. Conversely, exposure to PFOS induced an overproduction of a Cu-Zn superoxide dismutase (A0A7J6G1D4) hemp leaves, pointing to a possible accumulation of superoxide anion ($O_2^{\cdot-}$) as one of the mechanisms underlying PFOS-induced phytotoxicity.

5. Conclusions

This study evaluated morphological and physiological parameters, genotoxic endpoints and alterations in leaf proteome following PFAS accumulation in hemp shoots. The data revealed that shoot concentrations on the order of μg g^{-1} didn't result in evident morphological alterations. Although high aerial accumulation is a beneficial trait in the context of phytoremediation, this aspect should be considered as an ecological risk for possible trophic transfer, as shoots are potentially edible and easily accessible plant parts. PFOA, despite accumulating in hemp tissues at significantly lower concentrations than PFOS, induces

comparable levels of DNA damage and activates distinct metabolic pathways (Fig. 7), thus highlighting the importance of comparative studies in assessing PFAS genotoxicity. The results obtained suggested that the genotoxic effect may arise from a decrease in antioxidant enzyme activity with consequent oxidative stress, leading to an increase in DNA oxidation markers and genomic DNA fragmentation (Fig. 7). The latter may result directly from an increase in ROS within the nucleus, but also indirectly from incomplete repair of premutagenic 8-oxo-dG through the base excision repair mechanism, with possible formation and accumulation of single- and double-strand breaks. In addition, comparative proteomic analysis revealed a common response of both PFOA and PFOS on the chloroplast proteome and on proteins involved in redox homeostasis. Exposure to the two PFAAs also resulted in the disruption of specific biological processes. While PFOS accumulation decreased the abundance of proteins directly involved in gluconeogenesis, PFOA exposure promoted the synthesis of proteins involved in chlorophyll biosynthesis, suggesting that the two compounds may interact with different molecular targets. In the case of PFOA, the observed increase in biomass and chlorophyll content in the presence of genotoxic damage could represent an overcompensatory growth response triggered by deregulation of cellular homeostasis, although the molecular basis underlying this response remains to be elucidated. The present study has provided the first information on genotoxicity of PFAS in plant leaf tissues, providing also novel insights into the molecular mechanisms perturbated by PFAS from a proteomic perspective.

Environmental implication

Hemp is a candidate for PFAS phytoremediation, as it accumulates high concentrations of PFAS without showing visible signs of toxicity. Due to its features, it can be also a valuable model to understand possible genotoxic effects and alterations in cellular pathways induced by PFAS accumulation in plants. This study is among the first to investigate the genotoxic effects due to accumulation of PFOA and PFOS in plants, along with showing the alterations of cellular pathways induced by PFAS exposure. The study suggests hemp as a model species for environmental monitoring of PFAS and their detrimental effects on living organisms.

CRediT authorship contribution statement

Sophia Luche: Writing – original draft, Visualization, Investigation, Formal analysis, Data curation. **Alessandra Fanelli:** Writing – original draft, Formal analysis. **Annamaria Buschini:** Supervision, Methodology. **Ada Ricci:** Methodology. **Chiara Maccari:** Formal analysis. **Roberta Andreoli:** Methodology. **Teofilo Vamerali:** Supervision, Funding acquisition. **Patrizia Brunetti:** Supervision. **Giuseppe Capobianco:** Supervision. **Giovanna Visioli:** Writing – review & editing, Writing – original draft, Supervision, Project administration, Investigation, Conceptualization.

Funding

PRIN2022 Funded by the European Union- NextGenerationEU- under the National Recovery and Resilience Plan (NRRP), Mission 4, Component 2, Investment 1.1 call for tender No.104/2022 by the Italian Ministry of University and Research (MUR) - CUP B53D23017010006.

Declaration of Competing Interest

The authors declare that they have no known competing financial interests or personal relationships that could have appeared to influence the work reported in this paper.

Acknowledgement

This work has benefited from the equipment and framework of the COMPHUB and COMP-R Initiatives, funded by the 'Departments of Excellence' program of the Italian Ministry for University and Research (MIUR, 2018–2022 and MUR, 2023–2027). The authors acknowledged Dr. Caterina Frati (University of Parma) for helping with microscopy analyses, Dr. Ilaria Battisti (University of Padua) for her assistance with proteomic analyses, and Dr. Anna Rita Trentin (University of Padua) for PFAS quantification.

Appendix A. Supporting information

Supplementary data associated with this article can be found in the online version at doi:10.1016/j.jhazmat.2025.140686.

Data availability

Data are provided within the Supplementary materials.

References

[1] OECD, 2021. Reconciling Terminology of the Universe of Per- and Polyfluoroalkyl Substances: Recommendations and Practical Guidance. OECD Series on Risk Management of Chemicals. https://doi.org/10.1787/e458e796-en.
[2] Schymanski, E.L., Zhang, J., Thiessen, P.A., Chirsir, P., Kondic, T., Bolton, E.E., 2023. Per- and polyfluoroalkyl substances (PFAS) in PubChem: 7 million and growing. Environ Sci Technol 57, 16918–16928. https://doi.org/10.1021/acs.est.3c04855.
[3] Buck, R.C., Franklin, J., Berger, U., Conder, J.M., Cousins, I.T., de Voogt, P., Jensen, A.A., Kannan, K., Mabury, S.A., van Leeuwen, S.P.J., 2011. Perfluoroalkyl and polyfluoroalkyl substances in the environment: Terminology, classification, and origins. Integr Environ Assess Manag 7, 513–541. https://doi.org/10.1002/ieam.258.
[4] Brunn, H., Arnold, G., Körner, W., Rippen, G., Steinhäuser, K.G., Valentin, I., 2023. PFAS: forever chemicals—persistent, bioaccumulative and mobile. Reviewing the status and the need for their phase out and remediation of contaminated sites. Environ Sci Eur 35, 20. https://doi.org/10.1186/s12302-023-00721-8.
[5] Evich, M.G., Davis, M.J.B., McCord, J.P., Acrey, B., Awkerman, J.A., Knappe, D.R. U., Lindstrom, A.B., Speth, T.F., Tebes-Stevens, C., Strynar, M.J., Wang, Z., Weber, E.J., Henderson, W.M., Washington, J.W., 2022. Per- and polyfluoroalkyl substances in the environment. Science 375, eabg9065. https://doi.org/10.1126/science.abg9065.
[6] Fenton, S.E., Ducatman, A., Boobis, A., DeWitt, J.C., Lau, C., Ng, C., Smith, J.S., Roberts, S.M., 2021. Per- and Polyfluoroalkyl substance toxicity and human health review: current state of knowledge and strategies for informing future research. Environ Toxicol Chem 40, 606–630. https://doi.org/10.1002/etc.4890.
[7] Ma, T., Pan, X., Wang, T., Li, X., Luo, Y., 2023. Toxicity of per- and polyfluoroalkyl substances to nematodes. Toxics 11. https://doi.org/10.3390/toxics11070593.
[8] Pandelides, Z., Conder, J., Choi, Y., Allmon, E., Hoskins, T., Lee, L., Hoverman, J., Sepúlveda, M., 2023. A critical review of amphibian per- and polyfluoroalkyl substance ecotoxicity research studies: identification of screening levels in water and other useful resources for site-specific ecological risk assessments. Environ Toxicol Chem 42, 2078–2090. https://doi.org/10.1002/etc.5695.
[9] Panieri, E., Baralic, K., Djukic-Cosic, D., Djordjevic, A.B., Saso, L., 2022. PFAS molecules: a major concern for the human health and the environment. Toxics 10, 1–55. https://doi.org/10.3390/toxics10020044.
[10] de Souza, C.P., Guedes T de, A., Fontanetti, C.S., 2016. Evaluation of herbicides action on plant bioindicators by genetic biomarkers: a review. Environ Monit Assess 188. https://doi.org/10.1007/s10661-016-5702-8.
[11] Kwasniewska, J., Bara, A.W., 2022. Plant Cytogenetics in the micronuclei investigation—The past, current status, and perspectives. Int J Mol Sci 23. https://doi.org/10.3390/ijms23031306.
[12] Alias, C., Feretti, D., Benassi, L., Zerbini, I., Zani, C., Sorlini, S., 2023. Tools for monitoring toxicological and genotoxicological changes in a drinking water treatment plant in Northeast Italy. Water Environ J 37, 81–94. https://doi.org/10.1111/wej.12819.
[13] Sivaram, A.K., Logeshwaran, P., Surapaneni, A., Shah, K., Crosbie, N., Rogers, Z., Lee, E., Venkatraman, K., Kannan, K., Naidu, R., Megharaj, M., 2021. Evaluation of cyto-genotoxicity of perfluorooctane sulfonate (PFOS) to Allium cepa. Environ Toxicol Chem 40, 792–798. https://doi.org/10.1002/etc.4905.
[14] Adu, O., Ma, X., Sharma, V.K., 2023. Bioavailability, phytotoxicity and plant uptake of per-and polyfluoroalkyl substances (PFAS): A review. J Hazard Mater 447, 130805. https://doi.org/10.1016/j.jhazmat.2023.130805.
[15] Li, S., Wang, L., Li, J., Gao, Y., Wen, S., Yao, J., Zhu, L., Wang, J., Guan, E., Kim, Y.M., Wang, J., 2025. Migration characteristics and toxic effects of perfluorooctane sulfonate and perfluorobutane sulfonate in tobacco. Sci Total Environ 961, 178405. https://doi.org/10.1016/j.scitotenv.2025.178405.
[16] Zhang, P., Sun, L., Liu, F., Gao, Q., Wang, R., Ju, Q., Xu, J., 2022. Perfluorooctanoic acid and perfluorooctane sulfonic acid inhibit plant growth through the modulation of phytohormone signalling pathways: evidence from

molecular and genetic analysis in Arabidopsis. Sci Total Environ 851, 158287. https://doi.org/10.1016/j.scitotenv.2022.158287.
[17] Li, P., Oyang, X., Xie, X., Li, Z., Yang, H., Xi, J., Guo, Y., Tian, X., Liu, B., Li, J., Xiao, Z., 2020. Phytotoxicity induced by perfluorooctanoic acid and perfluorooctane sulfonate via metabolomics. J Hazard Mater 389, 121852. https://doi.org/10.1016/j.jhazmat.2019.121852.
[18] Ghisi, R., Vamerali, T., Manzetti, S., 2019. Accumulation of perfluorinated alkyl substances (PFAS) in agricultural plants: A review. Environ Res 169, 326–341. https://doi.org/10.1016/j.envres.2018.10.023.
[19] Gredelj, A., Nicoletto, C., Polesello, S., Ferrario, C., Valsecchi, S., Lava, R., Barausse, A., Zanon, F., Palmeri, L., Guidolin, L., Bonato, M., 2020. Uptake and translocation of perfluoroalkyl acids (PFAAs) in hydroponically grown red chicory (Cichorium intybus L.): Growth and developmental toxicity, comparison with growth in soil and bioavailability implications. Sci Total Environ 720, 137333. https://doi.org/10.1016/j.scitotenv.2020.137333.
[20] Li, J., Sun, J., Li, P., 2022. Exposure routes, bioaccumulation and toxic effects of per- and polyfluoroalkyl substances (PFASs) on plants: A critical review. Environ Int 158, 106891. https://doi.org/10.1016/j.envint.2021.106891.
[21] Marzi, D., Valente, F., Luche, S., Caissutti, C., Sabia, A., Capitani, I., Capobianco, G., Serranti, S., Masi, A., Panozzo, A., Ricci, A., Bolla, P.K., Vamerali, T., Brunetti, P., Visioli, G., 2025. Phytoremediation of perfluoroalkyl and polyfluoroalkyl substances (PFAS): Insights on plant uptake, omics analysis, contaminant detection and biomass disposal. Sci Total Environ 959. https://doi.org/10.1016/j.scitotenv.2024.178323.
[22] Nassazzi, W., Wu, T.C., Jass, J., Lai, F.Y., Ahrens, L., 2023. Phytoextraction of per- and polyfluoroalkyl substances (PFAS) and the influence of supplements on the performance of short–rotation crops. Environ Pollut 333, 122038. https://doi.org/10.1016/j.envpol.2023.122038.
[23] Nason, S.L., Thomas, S., Stanley, C., Silliboy, R., Blumenthal, M., Zhang, W., Liang, Y., Jones, J.P., Zuverza-Mena, N., White, J.C., Haynes, C.L., Vasiliou, V., Timko, M.P., Berger, B.W., 2024. A comprehensive trial on PFAS remediation: hemp phytoextraction and PFAS degradation in harvested plants. Environmental Science Advances 3, 304–313. https://doi.org/10.1039/d3va00340j.
[24] He, Q., Yan, Z., Qian, S., Xiong, T., Grieger, K.D., Wang, X., Liu, C., Zhi, Y., 2023. Phytoextraction of per- and polyfluoroalkyl substances (PFAS) by weeds: Effect of PFAS physicochemical properties and plant physiological traits. J Hazard Mater 454, 131492. https://doi.org/10.1016/j.jhazmat.2023.131492.
[25] Lesmeister, L., Lange, F.T., Breuer, J., Biegel-Engler, A., Giese, E., Scheurer, M., 2021. Extending the knowledge about PFAS bioaccumulation factors for agricultural plants - A review. Sci Total Environ 766, 142640. https://doi.org/10.1016/j.scitotenv.2020.142640.
[26] Qian, S., Lu, H., Xiong, T., Zhi, Y., Munoz, G., Zhang, C., Li, Z., Liu, C., Li, W., Wang, X., He, Q., 2023. Bioaccumulation of Per- and Polyfluoroalkyl Substances (PFAS) in Ferns: Effect of PFAS Molecular Structure and Plant Root Characteristics. Environ Sci Technol 57, 4443–4453. https://doi.org/10.1021/acs.est.2c06883.
[27] Wright, T., Crompton, M., Bishop, D., Currell, G., Suwal, L., Turner, B.D., 2024. Phytoremediation evaluation of forever chemicals using hemp (Cannabis sativa L.): Pollen bioaccumulation and the risk to bees. Chemosphere 370, 143859. https://doi.org/10.1016/j.chemosphere.2024.143859.
[28] Sharma, N., Barion, G., Shrestha, I., Ebinezer, L.B., Trentin, A.R., Vamerali, T., Mezzalira, G., Masi, A., Ghisi, R., 2020. Accumulation and effects of perfluoroalkyl substances in three hydroponically grown Salix L. species. Ecotoxicol Environ Saf 191. https://doi.org/10.1016/j.ecoenv.2019.110150.
[29] Kotecha, J.L., Ram, V.R., 2023. Extraction and Spectrophotometric Determination of Chlorophyll Content and Carotenoids from Cocos nucifera L. Leaf using Various Solvents in Saurashtra Region. Int J Plant Environ 9, 364–368. https://doi.org/10.18811/ijpen.v9i04.09.
[30] Potestio, S., Giannelli, G., Degola, F., Vamerali, T., Fragni, R., Cocconi, E., Sandei, L., Visioli, G., 2024. Salt stress mitigation and improvement in fruit nutritional characteristics of tomato plants: New opportunities from the exploitation of a halotorelant Agrobacterium strain. Plant Stress 13, 100558. https://doi.org/10.1016/j.stress.2024.100558.
[31] Gullì, M., Marchi, L., Fragni, R., Buschini, A., Visioli, G., 2018. Epigenetic modifications preserve the hyperaccumulator Noccaea caerulescens from Ni geno-toxicity. Environ Mol Mutagen 59, 464–475. https://doi.org/10.1002/em.22191.
[32] Carpentier, S.C., Witters, E., Laukens, K., Deckers, P., Swennen, R., Panis, B., 2005. Preparation of protein extracts from recalcitrant plant tissues: An evaluation of different methods for two-dimensional gel electrophoresis analysis. Proteomics 5, 2497–2507. https://doi.org/10.1002/pmic.200401222.
[33] Battisti, I., Ebinezer, L.B., Lomolino, G., Masi, A., Arrigoni, G., 2021. Protein profile of commercial soybean milks analyzed by label-free quantitative proteomics. Food Chem 352. https://doi.org/10.1016/j.foodchem.2021.129299.
[34] Cox, J., Mann, M., 2008. MaxQuant enables high peptide identification rates, individualized p.p.b.-range mass accuracies and proteome-wide protein quantification. Nat Biotechnol 26, 1367–1372. https://doi.org/10.1038/nbt.1511.
[35] Willforss, J., Chawade, A., Levander, F., 2019. NormalyzerDE: Online Tool for Improved Normalization of Omics Expression Data and High-Sensitivity Differential Expression Analysis. J Proteome Res 18, 732–740. https://doi.org/10.1021/acs.jproteome.8b00523.
[36] Cantalapiedra, C.P., Hernandez-Plaza, A., Letunic, I., Bork, P., Huerta-Cepas, J., 2021. eggNOG-mapper v2: Functional Annotation, Orthology Assignments, and Domain Prediction at the Metagenomic Scale. Mol Biol Evol 38, 5825–5829. https://doi.org/10.1093/molbev/msab293.
[37] Larsson, J., 2024. {eulerr}: Area-Proportional Euler and. Venn Diagr Ellipses.
[38] Wickham, H., 2016. ggplot2: Elegant Graphics for Data Analysis. Springer-Verlag New York.
[39] Gu, Z., Gu, L., Eils, R., Schlesner, M., Brors, B., 2014. circlize Implements and enhances circular visualization in R. Bioinformatics 30, 2811–2812. https://doi.org/10.1093/bioinformatics/btu393.
[40] Johnson, G.R., Brusseau, M.L., Carroll, K.C., Tick, G.R., Duncan, C.M., 2022. Global distributions, source-type dependencies, and concentration ranges of per- and polyfluoroalkyl substances in groundwater. Sci Total Environ 841, 156602. https://doi.org/10.1016/j.scitotenv.2022.156602.
[41] Kookana, R.S., Sha, B., Baluyot, J.C., Bowles, K.C., Kah, M., Padhye, L.P., Ying, G. G., Navarro, D., Velarde, M.C., Higgins, C.P., Cousins, I.T., 2025. Human exposure to per- and poly-fluoroalkyl substances (PFAS) in Asia and contributing factors, with a focus on East Asia. Environ Sci Process Impacts 27, 2614–2635. https://doi.org/10.1039/d5em00396b.
[42] Felizeter, S., Jürling, H., Kotthoff, M., De Voogt, P., McLachlan, M.S., 2020. Influence of soil on the uptake of perfluoroalkyl acids by lettuce: A comparison between a hydroponic study and a field study. Chemosphere 260, 127608. https://doi.org/10.1016/j.chemosphere.2020.127608.
[43] Zhang, D., Zhang, W., Liang, Y., 2019. Distribution of eight perfluoroalkyl acids in plant-soil-water systems and their effect on the soil microbial community. Sci Total Environ 697, 134146. https://doi.org/10.1016/j.scitotenv.2019.134146.
[44] Xu, J., Ren, H., Liu, Z., Sun, H., Shang, J., Tan, W., Cui, Q., Liu, S., Sun, X., 2024. Differential uptake and translocation of perfluoroalkyl substances by vegetable roots and leaves: Insight into critical influencing factors. Sci Total Environ 949. https://doi.org/10.1016/j.scitotenv.2024.175205.
[45] Silva, J.A.K., Martin, W.A., McCray, J.E., 2021. Air-water interfacial adsorption coefficients for PFAS when present as a multi-component mixture. J Contam Hydrol 236, 103731. https://doi.org/10.1016/j.jconhyd.2020.103731.
[46] Hearon, S.E., Orr, A.A., Moyer, H., Wang, M., Tamamis, P., Phillips, T.D., 2022. Montmorillonite clay-based sorbents decrease the bioavailability of per- and polyfluoroalkyl substances (PFAS) from soil and their translocation to plants. Environ Res 205. https://doi.org/10.1016/j.envres.2021.112433.
[47] Bizkarguenaga, E., Zabaleta, I., Prieto, A., Fernández, L.A., Zuloaga, O., 2016. Uptake of 8:2 perfluoroalkyl phosphate diester and its degradation products by carrot and lettuce from compost-amended soil. Chemosphere 152, 309–317. https://doi.org/10.1016/j.chemosphere.2016.02.130.
[48] Chen, Z., Hua, Z., Guo, P., 2024. The bioaccumulation and ecotoxicity of co-exposure of per(poly)fluoroalkyl substances and polystyrene microplastics to Eichhornia crassipes. Water Res 260. https://doi.org/10.1016/j.watres.2024.121878.
[49] Awad, J., Brunetti, G., Juhasz, A., Williams, M., Navarro, D., Drigo, B., Bougoure, J., Vanderzalm, J., Beecham, S., 2022. Application of native plants in constructed floating wetlands as a passive remediation approach for PFAS-impacted surface water. J Hazard Mater 429. https://doi.org/10.1016/j.jhazmat.2022.128326.
[50] Wen, B., Li, L., Liu, Y., Zhang, H., Hu, X., Shan, X., Zhang, S., 2013. Mechanistic studies of perfluorooctane sulfonate, perfluorooctanoic acid uptake by maize (Zea mays L. cv. TY2). Plant Soil 370, 345–354. https://doi.org/10.1007/s11104-013-1637-9.
[51] Xu, Z., Tang, T., Cheng, H., Bao, Q., Yu, J., Zhang, C., Wu, T., Zhao, X., Schramm, K.W., Wang, Y., 2019. Negligible effects of TiO2 nanoparticles at environmentally relevant concentrations on the translocation and accumulation of perfluorooctanoic acid and perfluorooctanesulfonate in hydroponically grown pumpkin seedlings (Cucurbita maxima × C. moschata). Sci Total Environ 686, 171–178. https://doi.org/10.1016/j.scitotenv.2019.05.473.
[52] Wattier, B.D., Gonzales, A.K., Martinez, N.E., 2023. Perfluorooctanoic acid uptake in the mustard species Brassica juncea. J Environ Qual 52, 199–206. https://doi.org/10.1002/jeq2.20431.
[53] Yu, P.F., Xiang, L., Li, X.H., Ding, Z.R., Mo, C.H., Li, Y.W., Li, H., Cai, Q.Y., Zhou, D.M., Wong, M.H., 2018. Cultivar-Dependent Accumulation and Translocation of Perfluorooctanesulfonate among Lettuce (Lactuca sativa L.) Cultivars Grown on Perfluorooctanesulfonate-Contaminated Soil. J Agric Food Chem 66, 13096–13106. https://doi.org/10.1021/acs.jafc.8b04548.
[54] Xiang, L., Chen, L., Yu, L.Y., Yu, P.F., Zhao, H.M., Mo, C.H., Li, Y.W., Li, H., Cai, Q.Y., Zhou, D.M., Wong, M.H., 2018. Genotypic variation and mechanism in uptake and translocation of perfluorooctanoic acid (PFOA) in lettuce (Lactuca sativa L.) cultivars grown in PFOA-polluted soils. Sci Total Environ 636, 999–1008. https://doi.org/10.1016/j.scitotenv.2018.04.354.
[55] Zhao, H.M., Du, H., Xiang, L., Chen, Y.L., Lu, L.A., Li, Y.W., Li, H., Cai, Q.Y., Mo, C.H., 2015. Variations in phthalate ester (PAE) accumulation and their formation mechanism in Chinese flowering cabbage (Brassica parachinensis L.) cultivars grown on PAE-contaminated soils. Environ Pollut 206, 95–103. https://doi.org/10.1016/j.envpol.2015.06.008.
[56] Velini, E.D., Alves, E., Godoy, M.C., Meschede, D.K., Souza, R.T., Duke, S.O., 2008. Glyphosate applied at low doses can stimulate plant growth. Pest Manag Sci 64, 489–496. https://doi.org/10.1002/ps.1562.
[57] Tang, Y.-T., Qiu, R.-L., Zeng, X.-W., Ying, R.-R., Yu, F.-M., Zhou, X.-Y., 2009. Lead, zinc, cadmium hyperaccumulation and growth stimulation in Arabis paniculata Franch. Environ Exp Bot 66, 126–134. https://doi.org/10.1016/j.envexpbot.2008.12.016.
[58] Hashmi, M.Z., Naveedullah, Shen, H., Zhu, S., Yu, C., Shen, C., 2014. Growth, bioluminescence and shoal behavior hormetic responses to inorganic and/or organic chemicals: a review. Environ Int 64, 28–39. https://doi.org/10.1016/j.envint.2013.11.018.

[59] Erofeeva, E.A., 2022. Hormesis in plants: Its common occurrence across stresses. Curr Opin Toxicol 30, 100333. https://doi.org/10.1016/j.cotox.2022.02.006.
[60] Agathokleous, E., Feng, Z.Z., Peñuelas, J., 2020. Chlorophyll hormesis: Are chlorophylls major components of stress biology in higher plants? Sci Total Environ 726, 138637. https://doi.org/10.1016/j.scitotenv.2020.138637.
[61] Li, X., Wang, Z., Ge, Y., Sun, H., Zhang, L., 2023. Comparative stress response assessment of PFOS and its alternatives, F-53B and OBS, in wheat: An insight of toxic mechanisms and relative magnitudes. Ecotoxicol Environ Saf 263, 115333. https://doi.org/10.1016/j.ecoenv.2023.115333.
[62] Li, R., Tang, T., Qiao, W., Huang, J., 2020. Toxic effect of perfluorooctane sulfonate on plants in vertical-flow constructed wetlands. J Environ Sci (China) 92, 176–186. https://doi.org/10.1016/j.jes.2020.02.018.
[63] Li, Q., Xiao, Y., Zhang, W., Li, S., Liu, J., Yu, Y., Wen, Y., Zhang, Y., Lei, N., Wang, Q., 2023. Single and combined toxicity effects of microplastics and perfluorooctanoic acid on submerged macrophytes and biofilms. Sci Total Environ 897. https://doi.org/10.1016/j.scitotenv.2023.165370.
[64] Soares, L.O.S., de Araujo, G.F., Gomes, T.B., Júnior, S.F.S., Cuprys, A.K., Soares, R.M., Saggioro, E.M., 2025. Antioxidant system alterations and oxidative stress caused by polyfluoroalkyl substances (PFAS) in exposed biota: a review. Sci Total Environ 977, 179395. https://doi.org/10.1016/j.scitotenv.2025.179395.
[65] Chen, J.C., Baumert, B.O., Li, Y., Li, Y., Pan, S., Robinson, S., Rubbo, B., Costello, E., He, J., Hampson, H., Beglarian, E., Rock, S., Goodrich, J.A., Eckel, S. P., Aung, M.T., McConnell, R., Conti, D.V., Chatzi, L., 2023. Associations of per- and polyfluoroalkyl substances, polychlorinated biphenyls, organochlorine pesticides, and polybrominated diphenyl ethers with oxidative stress markers: a systematic review and meta-analysis. Environ Res 239, 117308. https://doi.org/10.1016/j.envres.2023.117308.
[66] Sofo, A., Scopa, A., Nuzzaci, M., Vitti, A., 2015. Ascorbate Peroxidase and Catalase Activities and Their Genetic Regulation in Plants Subjected to Drought and Salinity Stresses. Int J Mol Sci 16, 13561–13578. https://doi.org/10.3390/ijms160613561.
[67] Fan, L., Tang, J., Zhang, D., Ma, M., Wang, Y., Han, Y., 2020. Investigations on the phytotoxicity of perfluorooctanoic acid in Arabidopsis thaliana. Environ Sci Pollut Res Int 27, 1131–1143. https://doi.org/10.1007/s11356-019-07018-5.
[68] Pan, Y., Wen, B., Zhang, H., Zhang, S., 2021. Comparison of 6:2 chlorinated polyfluorinated ether sulfonate (6:2 Cl-PFESA) and perfluorooctane sulfonate (PFOS) accumulation and toxicity in mung bean. Environ Pollut 287. https://doi.org/10.1016/j.envpol.2021.117332.
[69] Liu, Y., Jin, T., Wang, L., Tang, J., 2023. Polystyrene micro and nanoplastics attenuated the bioavailability and toxic effects of Perfluorooctane sulfonate (PFOS) on soybean (Glycine max) sprouts. J Hazard Mater 448. https://doi.org/10.1016/j.jhazmat.2023.130911.
[70] Xu, M., Wan, J., Niu, Q., Liu, R., 2019. PFOA and PFOS interact with superoxide dismutase and induce cytotoxicity in mouse primary hepatocytes: A combined cellular and molecular methods. Environ Res 175, 63–70. https://doi.org/10.1016/j.envres.2019.05.008.
[71] Xu, M., Cui, Z., Zhao, L., Hu, S., Zong, W., Liu, R., 2018. Characterizing the binding interactions of PFOA and PFOS with catalase at the molecular level. Chemosphere 203, 360–367. https://doi.org/10.1016/j.chemosphere.2018.03.200.
[72] Rajak, P., Ganguly, A., 2023. The ligand-docking approach explores the binding affinity of PFOS and PFOA for major endogenous antioxidants: A potential mechanism to fuel oxidative stress. Sustain Chem Environ 4, 100047. https://doi.org/10.1016/j.scenv.2023.100047.
[73] Galati, S., DalCorso, G., Furini, A., Fragni, R., Maccari, C., Mozzoni, P., Giannelli, G., Buschini, A., Visioli, G., 2023. DNA methylation is enhanced during Cd hyperaccumulation in Noccaea caerulescens ecotype Ganges. Environ Sci Pollut Res 30, 26178–26190. https://doi.org/10.1007/s11356-022-23983-w.
[74] Giannelli, G., Mattarozzi, M., Gentili, S., Fragni, R., Maccari, C., Andreoli, R., Visioli, G., 2024. A novel PGPR strain homologous to Beijerinckia fluminensis induces biochemical and molecular changes involved in Arabidopsis thaliana salt tolerance. Plant Physiol Biochem 206, 108187. https://doi.org/10.1016/j.plaphy.2023.108187.
[75] Li, P., Oyang, X., Xie, X., Li, Z., Yang, H., Xi, J., Guo, Y., Tian, X., Liu, B., Li, J., Xiao, Z., 2020. Phytotoxicity induced by perfluorooctanoic acid and perfluorooctane sulfonate via metabolomics. J Hazard Mater 389, 121852. https://doi.org/10.1016/j.jhazmat.2019.121852.
[76] Kim, J.H., Park, H.Y., Jeon, J.D., Kho, Y., Kim, S.-K., Park, M.-S., Hong, Y.-C., 2016. The modifying effect of vitamin C on the association between perfluorinated compounds and insulin resistance in the Korean elderly: a double-blind, randomized, placebo-controlled crossover trial. Eur J Nutr 55, 1011–1020. https://doi.org/10.1007/s00394-015-0915-0.
[77] Lin, C.-Y., Lee, H.-L., Hwang, Y.-T., Su, T.-C., 2020. The association between total serum isomers of per- and polyfluoroalkyl substances, lipid profiles, and the DNA oxidative/nitrative stress biomarkers in middle-aged Taiwanese adults. Environ Res 182, 109064. https://doi.org/10.1016/j.envres.2019.109064.
[78] Ambroz, A., Rossner, P.J., Rossnerova, A., Honkova, K., Milcova, A., Pastorkova, A., Klema, J., Pulkrabova, J., Parizek, O., Vondraskova, V., Zelenka, J., Vrzáčková, N., Schmuczerova, J., Topinka, J., Sram, R.J., 2022. Oxidative STress and Antioxidant Response in Populations of the Czech Republic exposed to various levels of environmental pollutants. Int J Environ Res Public Health 19. https://doi.org/10.3390/ijerph19063609.
[79] Panneerselvan, L., Sivaram, A.K., Mallavarapu, M., Naidu, R., 2016. Evaluation of cyto- and genotoxic effects of Class B firefighting foam products: Tridol-S 3% AFFF and Tridol-S 6% AFFF to Allium cepa. Environ Technol Innov 6, 185–194. https://doi.org/10.1016/j.eti.2016.10.003.
[80] Sivaram, A.K., Lee, E., Curnow, A., Surapaneni, A., Kannan, K., Megharaj, M., 2023. Uptake, accumulation, and toxicity of per- and polyfluoroalkyl substances in Allium cepa grown in soils amended with biosolids. Environ Chall 10, 100670. https://doi.org/10.1016/j.envc.2022.100670.
[81] Yan, P.-F., Dong, S., Pennell, K.D., Cápiro, N.L., 2024. A review of the occurrence and microbial transformation of per- and polyfluoroalkyl substances (PFAS) in aqueous film-forming foam (AFFF)-impacted environments. Sci Total Environ 927, 171883. https://doi.org/10.1016/j.scitotenv.2024.171883.
[82] Logeshwaran, P., Sivaram, A.K., Surapaneni, A., Kannan, K., Naidu, R., Megharaj, M., 2021. Exposure to perfluorooctanesulfonate (PFOS) but not perfluorooctanoic acid (PFOA) at ppb concentration induces chronic toxicity in Daphnia carinata. Sci Total Environ 769, 144577. https://doi.org/10.1016/j.scitotenv.2020.144577.
[83] Ojo, A.F., Peng, C., Ng, J.C., 2022. Genotoxicity assessment of per- and polyfluoroalkyl substances mixtures in human liver cells (HepG2). Toxicology 482, 153359. https://doi.org/10.1016/j.tox.2022.153359.
[84] Wielsøe, M., Long, M., Ghisari, M., Bonefeld-Jørgensen, E.C., 2015. Perfluoroalkylated substances (PFAS) affect oxidative stress biomarkers in vitro. Chemosphere 129, 239–245. https://doi.org/10.1016/j.chemosphere.2014.10.014.
[85] Calabrese E.J.Evidence That Hormesis Represents an "' Overcompensation "' Response a Disrupt Homeost1999. 137135137.
[86] Ebinezer, L.B., Battisti, I., Sharma, N., Ravazzolo, L., Ravi, L., Trentin, A.R., Barion, G., Panozzo, A., Dall'Acqua, S., Vamerali, T., Quaggiotti, S., Arrigoni, G., Masi, A., 2022. Perfluorinated alkyl substances affect the growth, physiology and root proteome of hydroponically grown maize plants. J Hazard Mater 438, 129512. https://doi.org/10.1016/j.jhazmat.2022.129512.
[87] O'Hara, L., Longstaffe, J.G., 2023. 1H-nuclear magnetic resonance metabolomics analysis of arabidopsis thaliana exposed to perfluorooctanoic acid and perfluoroctanesulfonic acid. Environ Toxicol Chem 42, 663–672. https://doi.org/10.1002/etc.5547.
[88] Guo, Q., He, Z., Liu, X., Liu, B., Zhang, Y., 2020. High-throughput non-targeted metabolomics study of the effects of perfluorooctane sulfonate (PFOS) on the metabolic characteristics of A. thaliana leaves. Sci Total Environ 710, 135542. https://doi.org/10.1016/j.scitotenv.2019.135542.
[89] Du, W., Liu, X., Zhao, L., Xu, Y., Yin, Y., Wu, J., Ji, R., Sun, Y., Guo, H., 2020. Response of cucumber (Cucumis sativus) to perfluorooctanoic acid in photosynthesis and metabolomics. Sci Total Environ 724, 138257. https://doi.org/10.1016/j.scitotenv.2020.138257.
[90] Li, P., Sun, J., Xie, X., Li, Z., Huang, B., Zhang, G., Li, J., Xiao, Z., 2021. Stress response and tolerance to perfluorooctane sulfonate (PFOS) in lettuce (Lactuca sativa). J Hazard Mater 404. https://doi.org/10.1016/j.jhazmat.2020.124213.
[91] Li, P., Xiao, Z., Xie, X., Li, Z., Yang, H., Ma, X., Sun, J., Li, J., 2021. Perfluorooctanoic acid (PFOA) changes nutritional compositions in lettuce (Lactuca sativa) leaves by activating oxidative stress. Environ Pollut 285. https://doi.org/10.1016/j.envpol.2021.117246.
[92] Yokoyama, R., de Oliveira, M.V.V., Kleven, B., Maeda, H.A., 2021. The entry reaction of the plant shikimate pathway is subjected to highly complex metabolite-mediated regulation. Plant Cell 33, 671–696. https://doi.org/10.1093/plcell/koaa042.
[93] Li, P., Oyang, X., Xie, X., Guo, Y., Li, Z., Xi, J., Zhu, D., Ma, X., Liu, B., Li, J., Xiao, Z., 2020. Perfluorooctanoic acid and perfluorooctane sulfonate co-exposure induced changes of metabolites and defense pathways in lettuce leaves. Environ Pollut 256, 113512. https://doi.org/10.1016/j.envpol.2019.113512.
[94] de la Osa, C., Pérez-López, J., Feria, A.-B., Baena, G., Marino, D., Coleto, I., Pérez-Montaño, F., Gandullo, J., Echevarría, C., García-Mauriño, S., Monreal, J.A., 2022. Knock-down of phosphoenolpyruvate carboxylase 3 negatively impacts growth, productivity, and responses to salt stress in sorghum (Sorghum bicolor L.). Plant J 111, 231–249. https://doi.org/10.1111/tpj.15789.
[95] Huang, Y.-X., Yin, Y.-G., Sanuki, A., Fukuda, N., Ezura, H., Matsukura, C., 2015. Phosphoenolpyruvate carboxykinase (PEPCK) deficiency affects the germination, growth and fruit sugar content in tomato (Solanum lycopersicum L.). Plant Physiol Biochem 96, 417–425. https://doi.org/10.1016/j.plaphy.2015.08.021.
[96] Yang, Z., Shen, L., Hu, L., Cai, Y., Zheng, Q., Wu, Y., 2024. The PEPCK and FBP genes regulate gluconeogenesis metabolism in grape berries in response to light intensity. Horticulturae 10. https://doi.org/10.3390/horticulturae10121270.
[97] Ofoegbu, P.C., Wagner, D.C., Abolade, O., Clubb, P., Dobbs, Z., Sayers, I., Zenobio, J.E., Adeleye, A.S., Rico, C.M., 2022. Impacts of perfluorooctanesulfonic acid on plant biometrics and grain metabolomics of wheat (Triticum aestivum L.). J Hazard Mater Adv 7, 100131. https://doi.org/10.1016/j.hazadv.2022.100131.
[98] Busch, A.W.U., Montgomery, B.L., 2015. Interdependence of tetrapyrrole metabolism, the generation of oxidative stress and the mitigative oxidative stress response. Redox Biol 4, 260–271. https://doi.org/10.1016/j.redox.2015.01.010.
[99] Schlicke, H., Hartwig, A.S., Firtzlaff, V., Richter, A.S., Glässer, C., Maier, K., Finkemeier, I., Grimm, B., 2014. Induced deactivation of genes encoding chlorophyll biosynthesis enzymes disentangles tetrapyrrole-mediated retrograde signaling. Mol Plant 7, 1211–1227. https://doi.org/10.1093/mp/ssu034.
[100] Sevilla, F., Martí, M.C., De Brasi-Velasco, S., Jiménez, A., 2023. Redox regulation, thioredoxins, and glutaredoxins in retrograde signalling and gene transcription. J Exp Bot 74, 5955–5969. https://doi.org/10.1093/jxb/erad270.
[101] Li, H., Hu, H., Cao, L., Zhuo, Y., Wang, L., Ma, H., Zhong, M., 2025. Genome-wide characterization and expression analysis of the JRL gene family in response to

hormones and abiotic stress in tomato (Solanum lycopersicum L.). PeerJ 13, e19724. https://doi.org/10.7717/peerj.19724.
[102] Gao, Q., Yin, X., Wang, F., Zhang, C., Xiao, F., Wang, H., Hu, S., Liu, W., Zhou, S., Chen, L., Dai, X., Liang, M., 2023. Jacalin-related lectin 45 (OsJRL45) isolated from 'sea rice 86' enhances rice salt tolerance at the seedling and reproductive stages. BMC Plant Biol 23, 553. https://doi.org/10.1186/s12870-023-04533-z.
[103] Zhu, Y., Gao, F., 2025. Involvement of pathogenesis-related proteins and their roles in abiotic stress responses in plants. Biomolecules 15. https://doi.org/10.3390/biom15081103.